Mnin restraining stepover – evidence of significant Cretaceous–Cenozoic dextral strike-slip faulting along the Teisseyre-Tornquist Zone?

ANDRZEJ KONON[1*], SZYMON OSTROWSKI[2], BARBARA RYBAK-OSTROWSKA[1], MIROSŁAW LUDWINIAK[1], MICHAŁ ŚMIGIELSKI[1], MICHAŁ WYGLĄDAŁA[1], JOANNA URODA[1], SEBASTIAN KOWALCZYK[1], RADOSŁAW MIESZKOWSKI[1] and AGNIESZKA KŁOPOTOWSKA[1]

[1*]*Faculty of Geology, University of Warsaw, Al. Żwirki i Wigury 93, PL-02-089 Warszawa, Poland.*
[*] *E-mail: andrzej.konon@uw.edu.pl*
[2]*Polish Geological Institute –National Research Institute, Rakowiecka 4, PL-00-975 Warszawa, Poland.*

ABSTRACT:

Konon, A., Ostrowski, S., Rybak-Ostrowska, B., Ludwiniak, M., Śmigielski, M., Wyglądała, M., Uroda, J., Kowalczyk, S., Mieszkowski, R. and Kłopotowska, A. 2016. Mnin restraining stepover – evidence of significant Cretaceous–Cenozoic dextral strike-slip faulting along the Teisseyre-Tornquist Zone? *Acta Geologica Polonica*, **66** (3), 429–449. Warszawa.

A newly recognized Mnin restraining stepover is identified in the Permo-Mesozoic cover of the western part of the Late Palaeozoic Holy Cross Mountains Fold Belt (Poland), within a fault pattern consisting of dextral strike-slip faults. The formation of a large contractional structure at the Late Cretaceous – Cenozoic transition displays the significant role of strike-slip faulting along the western border of the Teisseyre-Tornquist Zone, in the foreland of the Polish part of the Carpathian Orogen. Theoretical relationships between the maximum fault offsets/mean step length, as well as between the maximum fault offsets/mean step width allowed the estimation of the values of possible offsets along the Snochowice and Mieczyn faults forming the Mnin stepover. The estimated values suggest displacements of as much as several tens of kilometres. The observed offset along the Tokarnia Fault and theoretical calculations suggest that the strike-slip faults west of the Late Palaeozoic Holy Cross Mountains Fold Belt belong to a large strike-slip fault system.

We postulate that the observed significant refraction of the faults forming the anastomosing fault pattern is related also to the interaction of the NW-SE-striking faults formed along the western border of the Teisseyre-Tornquist Zone and the reactivated WNW-ESE-striking faults belonging to the fault systems of the northern margin of the Tethys Ocean.

Keywords: Strike-slip fault pattern; Restraining stepover; Permo-Mesozoic cover; Holy Cross Mountains Fold Belt.

INTRODUCTION

Progress in the recognition of strike-slip structures that began about 60 years ago has allowed the identification of different extensional and contractional structures associated with strike-slip faulting all over the world. The investigations have shown that strike-slip faulting plays a significant role in intercontinental deformation within e.g., collisional 'mobile' belts and inverted sedimentary basins (for discussion see e.g., Moody and Hill 1956; Sylvester 1988; Woodcock and Schubert 1994 and citations therein). Strike-slip structures need the precise identification of diagnostic tectonic structures that formed as a result of the strike-
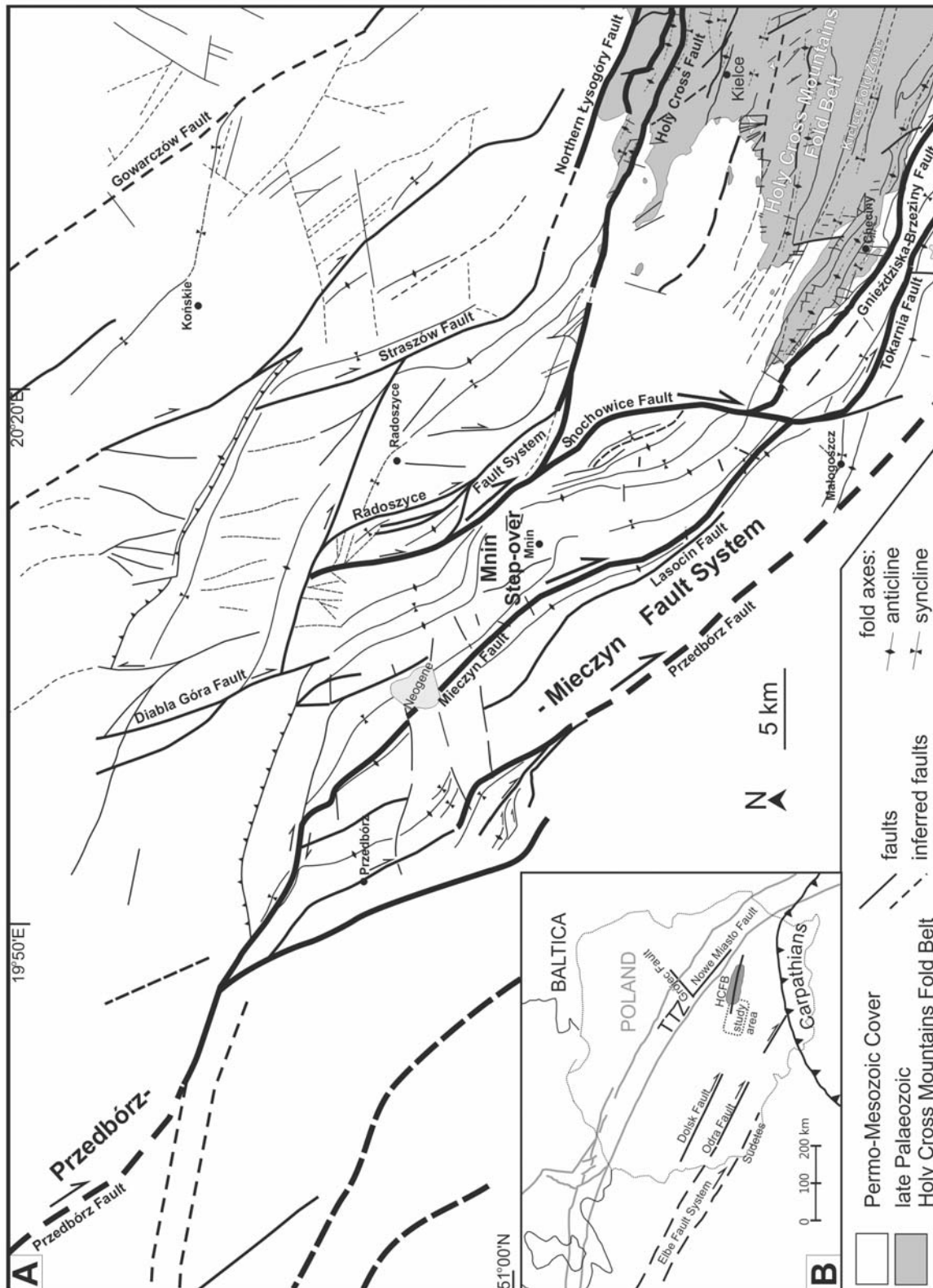
Text-fig. 1. A – Fault pattern within the Permo-Mesozoic cover of the western part of the Late Palaeozoic Holy Cross Mountains Fold Belt (Poland) (based on Czarnocki 1938, 1961; Jurkiewiczowa 1961; Krajewski 1961; Różycki 1961; Jurkiewicz 1965; Filonowicz 1967; Grzybowski and Kutek 1967; Jurkiewicz 1967; Hakenberg 1973; Szajn 1977, 1980, 1983; Kwapisz 1983; Filonowicz and Lindner 1986; Cieśla and Lindner 1990; Janiec 1991; Mastella and Konon 2002; Konon 2007, modified). B – Location of the study area

slip movements, as e.g., restraining (contractional) and releasing (extensional) stepovers or bends along the major fault (Woodcock and Fisher 1986; Woodcock and Schubert 1994; McClay and Bonora 2001; Wakabayashi *et al*. 2004; Wakabayashi 2007).

Restraining stepovers form in response to transpressional stress. Concentrations of lower and large-magnitude earthquake epicentres may be observed within restraining stepovers all of the world. For example, one of the famous earthquakes, the M 7.9 1906 San Francisco, California earthquake is likely to have nucleated in a stepover structure (Zoback *et al*. 1999; Oglesby 2005). Another example comes from the Indes-Qom stepover, where analysis of the earthquake focal mechanisms (for >Mw 5) revealed dextral oblique thrusting along the northern margin of the Sanandaj-Sirjan Zone within the restraining stepover zone (Morley *et al*. 2009; Babaahmadi *et al*. 2010).

Other structures useful for the precise identification of strike-slip movements in vertical cross-sections and on seismic profiles, as well as on geological maps and satellite images are: flower structures (e.g., Wilcox *et al*. 1973), folds with a helicoidal geometry of the ax-

ial surfaces in restraining stepovers (Sylvester 1988; Babaahmadi *et al*. 2010; Nadimi and Konon 2012), especially when they form an *en échelon* arrangement (Moody and Hill 1956; Jamison 1991; Woodcock and Schubert 1994), and vertical-axis rotated tectonic blocks bounded by major strike-slip faults (Woodcock and Fisher 1986; Mandl 1987; Sylvester 1988; Peacock *et al*. 1998; Woodcock and Rickards 2003; Kim *et al*. 2004; Konon 2007; Nadimi and Konon 2012). Apart from map-scale structures, identification of minor structures associated with major faults, such as slickensides observed within the near-surface parts of fault zones, horsetail splays, wing cracks or antithetic faults at the terminations of major faults, also demonstrate the presence of strike-slip movements.

The aim of this paper is to describe a newly discovered large-scale structure as a restraining stepover associated with dextral strike-slip faulting within the Permo-Mesozoic cover of the western part of the Late Palaeozoic Holy Cross Mountains Fold Belt (HCFB)

The contractional structure, termed the Mnin stepover, is discussed in the context of the activity of the main fault systems as a result of the inversion tectonics along the northern Peri-Tethyan Platform.
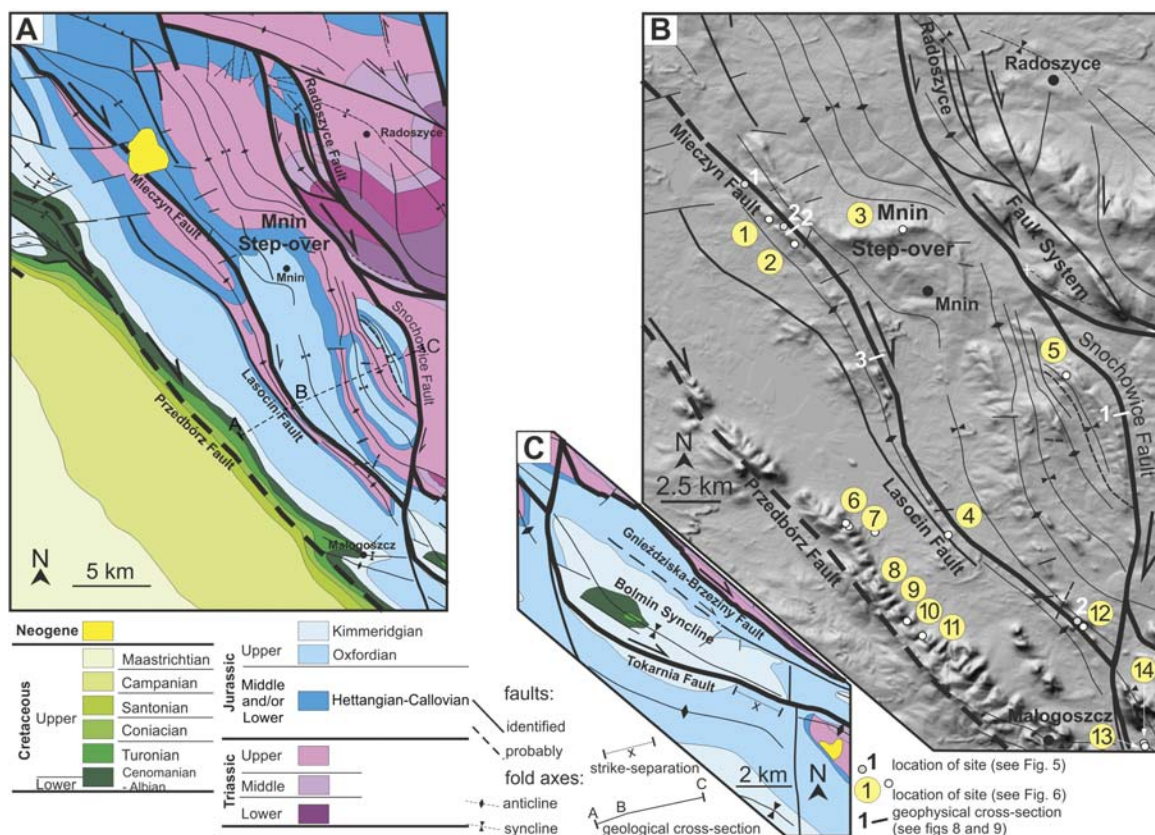
Text-fig. 2. A – Geological map of the Mnin stepover area (based on Czarnocki 1961; Jurkiewiczowa 1961; Krajewski 1961; Różycki 1961, modified). B – Simplified tectonic map of the Mnin stepover marked on a shaded-relief Shuttle Radar Topography Mission (SRTM) image. C – Geological map of the Bolmin Syncline area (based on Czarnocki 1961; Różycki 1961, modified)

GEOLOGICAL SETTING

The strike-slip fault pattern in the study area is developed within the Permo-Mesozoic cover, which unconformably overlies the Palaeozoic rocks of the Holy Cross Mountains Folded Belt (Text-figs 1, 2). The Holy Cross Mountains area is situated in the transition zone between the Polish and North German basins (e.g., Kutek and Głazek 1972; Ziegler 1982, 1990b; Dadlez *et al.* 1995, 1997; Krzywiec 2000, 2002; Kutek 2001; Dadlez 2003) and the northern Tethys shelf, from probably the Middle/Late Jurassic transition (Matyja 2009).

The Polish and North German basins formed along two regional zones of crustal weakness: the Teisseyre-Tornquist Zone (TTZ) and the Elbe Fault System (EFS), respectively (Text-fig. 1b) (e.g., Dadlez 1997; Scheck *et al.* 2002; Mazur *et al.* 2005; Scheck and Lamarche 2005). The study area is located near the western border of the NW-SE-striking Teisseyre-Tornquist Zone (TTZ), which represents a crustal-scale boundary that separates the East European Craton from the Palaeozoic Platform of Western Europe (e.g., Kutek and Głazek 1972; Pożaryski and Brochwicz-Lewiński 1978; Dadlez 1997; Dadlez *et al.* 1995, 1997; Dadlez 2006).

The significant role of strike-slip faulting during the inversion of the Polish Basin was suggested by e.g., Dadlez (1994), from analysis of the offsets of the folds, salt diapirs or synsedimentary grabens on geological maps; by Krzywiec (2000, 2002, 2009b) and Krzywiec *et al.* (2003, 2009), from the analysis of seismic profiles across the fault zones; and by Gutowski and Koyi (2007) from results of three-dimensional (3D) analogue models. The prevailing compressional/transpressional stress regime resulted in inversion tectonics at the end of the Cretaceous and the beginning of the Cenozoic along the northern Peri-Tethyan Platform (e.g., Ziegler 1987). Transmission of horizontal stress resulted from the collisional phases in the Alpine and Carpathian orogens, and additionally the Late Cretaceous Atlantic opening (e.g., Ziegler 1987, 1990a, b; Golonka *et al.* 2000; Dadlez 2003; Mazur *et al.* 2005).
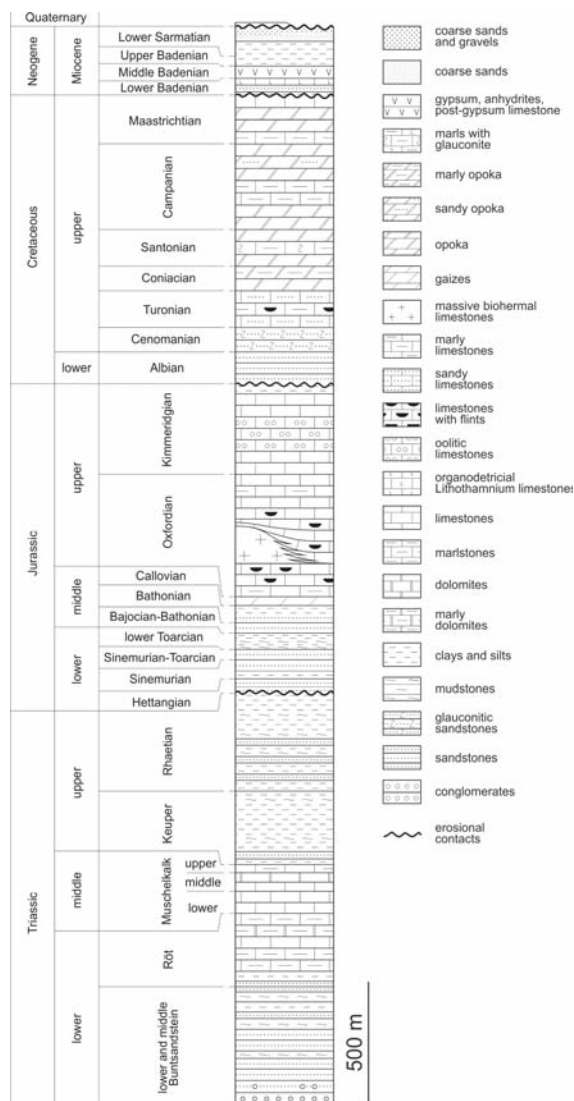
Mesozoic succession of the Permo-Mesozoic cover

The Mesozoic succession of the Permo-Mesozoic cover of the HCFB is composed of epicratonic sediments reaching a thickness of 2 to 4 km (Text-fig. 3). Triassic rocks rest upon the Palaeozoic basement characterized by a diverse morphology, usually on Middle and Upper Devonian rocks and only locally on Per-

mian strata. The lowermost part of the Triassic succession is built of clastic sediments: conglomerates, ferruginous quartz sandstones with mudstone interbeds, mudstones and claystones, and subordinately marls with interbeds of limestones, dolomites and anhydrites (Senkowiczowa 1961; Kuleta and Zbroja 2006). The thickness of the Lower Triassic is estimated at about 780 m (Jurkiewicz 1968; Szajn 1984). The clastic rocks are overlain by Middle Triassic pelitic limestones, with interbeds of dolomites, marls and claystones, with a thickness of about 140 m and 200 m in the south-western, and 200 m in the north-western part of the study area, respectively (Szajn 1984). The Upper Triassic comprises claystones and mudstones with interbeds of sandstones, marls, dolomites, anhydrites and gypsum, with a strongly variable thickness, from over 10 m to 700 m (Szajn 1984).

Sedimentation of Jurassic strata was preceded by erosion, indicated by erosional incisions within the Upper Triassic, which reach down to depth of several tens of metres (Jurkiewiczowa 1967). The Lower Jurassic is represented by largely terrestrial clastic sediments (Pieńkowski 1991, 2004; Świdrowska *et al*. 2008). They include gravels and conglomerates (Snochowice Beds), overlain by fine-grained quartz sandstones and mudstone-sandstone-claystone sediments with interbeds of siderites. Lack of the upper Toarcian indicates lack of continuous sedimentation between the Early and Middle Jurassic (Świdrowska *et al*. 2008; Matyja 2012). Lower Jurassic strata are preserved only in the north-eastern, northern and north-western part of the study area and their thickness varies from 58 m to about 800 m.

The Middle Jurassic is composed of clastic marine sediments passing into limestones (Matyja 2012). Clay sediments (Aalenian–Bajocian) occur solely within the north-eastern and northern part of the study area. Above occur white, fine-grained sandstones and siltstones with interbeds of limestones, ferruginous sands, detritic limestones and dark clays (Bajocian-Bathonian), and calcareous sandstones, sandy limestones with cherts and flints, gaizes and detritic limestones (Callovian) (Siemiątkowska-Giżejewska 1974; Giżejewska 1975; Barski 1999). In the zone of the studied fault network, the thickness of the Middle Jurassic does not exceed 150 m.

The Upper Jurassic is dominated by limestones (e.g., Kutek 1968; Matyja 1977; Matyja *et al.* 1996). The succession includes pelitic limestones and clay marls, medium- and thick-bedded limestones with flints, microbial-sponge limestones interbedded with thick-bedded limestones and marly limestones (Oxfordian). Above occur marls, oolite limestones, oyster

Text-fig. 3. Simplified lithostratigraphic log of the Mesozoic-Cenozoic succession of the HCFB cover (compiled and slightly modified from Jurkiewicz 1968; Hakenberg et al. 1976; Alexandrowicz et al. 1982; Szajn 1984; Filonowicz and Linder 1986; Czapowski 2004; Matyja 2012)

lumachells, marly clays and marls (Kimmeridgian) (Kutek 1968). The total thickness of the Upper Jurassic in the south-western part of the Permo-Mesozoic cover reaches slightly below 1100 m, and to the west of Mnin – about 870 m (Szajn 1984).

There is a stratigraphic gap between the Jurassic and Cretaceous (Senkowicz 1959; Kutek 1968; Hakenberg 1978). Kimmeridgian sediments are unconformably overlain by Lower Cretaceous sandstones, occasionally glauconitic sandstones, with interbeds of gaizes and spongiolites (Albian). The maximal thickness of the Lower Cretaceous in the study area reaches 130 m.

The Upper Cretaceous is represented by sandy limestones with gaizes, calcareous sandstones and conglomerates (Cenomanian); clays with flints and sandy limestones (Turonian); opokas, marls and gaizes (Turonian to Maastrichtian) (Marcinowski and Radwański 1983). The thickness of the Upper Cretaceous with the opokas of the lowermost Palaeocene reaches slightly above 1000 m.

In the southern and south-eastern part of the study area, the eroded, morphologically variable surface of Palaeozoic and Mesozoic rocks is covered by transgressive Miocene sediments of the Carpathian Foredeep Basin (Radwański 1969, 1973; Radwański and Górka 2012). The thickness of the Miocene strata does not exceed 300 m in the study area (Czapowski 2004).

Strike-slip fault pattern

The fault pattern within the Permo-Mesozoic cover and the HCFB is very complex and displays significant differences. Straight traces of faults dominate in the HCFB, whereas to the west of the HCFB, in the Permo-Mesozoic strata, the faults form an anastomosing fault pattern with prevailing non-planar faults (Text-fig. 1a) (Mastella and Konon 2002; Konon 2007, 2015).

The folds of the HCFB were formed after the Visean, probably during the late Carboniferous and before the late Permian (e.g., Czarnocki 1938, 1950).
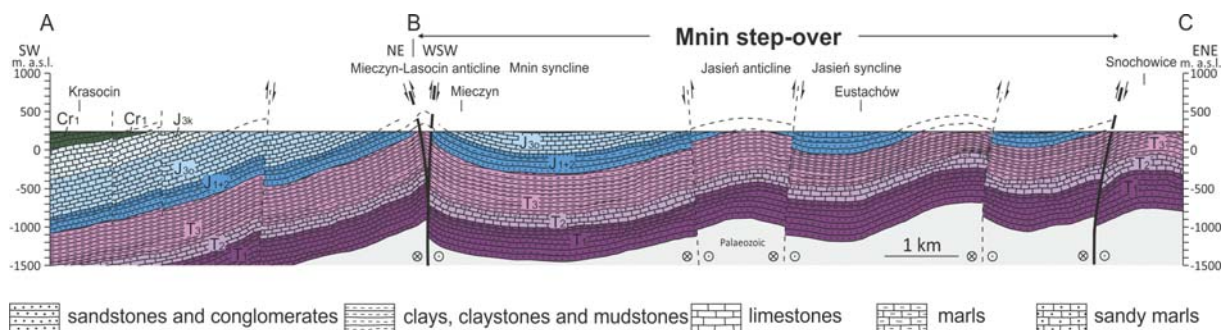
Text-fig. 4. Geological cross-section (based on Szajn 1983; Filonowicz and Lindner 1986, modified)

The folds are cut by map-scale, WNW-ESE-striking, longitudinal, and N-S to NNW-SSE-striking, transverse and oblique faults (Text-fig. 1a) (e.g., Czarnocki 1938; Konon 2007). The longitudinal fault traces are up to tens of kilometres long. The traces of the transverse and oblique faults are a few kilometres long. Strike-slip and shortening components prevail across the planes of longitudinal faults, whereas strike-slip, shortening and extension components may occur across transverse and oblique fault planes (e.g., Czarnocki 1950, 1956; Jaroszewski 1973, 1980; Mizerski 1991; Mizerski and Orłowski 1993; Konon and Śmigielski 2006; Konon 2007). A dextral strike-slip component dominated during the Late Palaeozoic (probably late Carboniferous and early Permian) along the major longitudinal faults, such as the Holy Cross Fault and the Northern Łysogóry Fault, when the shortening direction was approximately NW-SE-trending (Konon 2007; Szaniawski *et al.* 2011). Transmission of horizontal stress resulted from the collisional phases in the Variscan Orogen (*op. cit.*). The strike-slip fault network in the HCFB was later overprinted during the Maastrichtian/Palaeocene strike-slip stage of deformation (e.g., Jaroszewski 1972; Konon and Mastella 2001; Mastella and Konon 2002; Konon 2007).

Longitudinal faults, with axes parallel to Mesozoic–Cenozoic folds, dominate in the fault pattern within the Permo-Mesozoic strata overlying the lower Cambrian to lower Carboniferous rocks of the HCFB. NW-SE and NNW-SSE-striking faults, as well as WNW-SSE-striking faults, prevail west of the HCFB and south of the fold belt, respectively (Text-fig. 2) (Czarnocki 1938, 1948; Kutek and Głazek 1972; Stupnicka 1972; Konon and Mastella 2001; Mastella and Konon 2002; Konon 2015). Faults with several tens of kilometres-long traces were recognized as dip-slip faults (Text-figs 1b, 2 and 4) (Filonowicz 1967, 1968; Stupnicka 1972; Hakenberg 1973, 1974; Filonowicz and Lindner 1986). The possibility of the occurrence of a strike-slip component on their planes was also assumed (Kutek and Głazek 1972; Stupnicka 1972; Kowalski 1975; Pożaryski 1976; Konon and Mastella 2001; Mastella and Konon 2002). The strike-slip activity within the Permo-Mesozoic strata has already been recognized along the map-scale Gnieździska-Brzeziny Fault, with a several tens of kilometres-long trace (Konon and Mastella 2001; Mastella and Konon 2002) and along the faults forming the Mnin stepover (Konon *et al.* 2013, 2014; Konon 2015). The faults developed in the Maastrichtian/Palaeocene times when the maximum horizontal compressional stress S_{Hmax} was ~10° (Konon and Mastella 2001; Mastella and Konon 2002).

METHODS

Structural analysis

The analyses were made based on field observations in quarries and outcrops, geological maps, DEM-derived images of structures associated with strike-slip faults and geophysical investigations. The strike-slip component was identified based on the analysis of lineations on the slickensides and folds formed in the restraining stepover. Slickensides of first-order major faults and second-order minor faults consistent with Riedel shears as R and R' were noted along the strike-slip faults (Text-figs 5, 6 and 7).

Field mapping and near-surface geophysical methods based on electrical resistivity tomography (ERT) allowed for a detailed analysis of the broad fault zones (Text-figs 8 and 9).

Geophysical investigations

Geophysical investigations enabled the precise localization of the fault zones and the recognition of the shallow damage zones. The near-surface geophysical method ERT was applied for detailed imaging of three segments of the Mieczyn and Snochowice Fault zones, whose presence was evident from cartographic and geomorphologic data but which otherwise were poorly or randomly exposed in the outcrops (Text-fig. 2b).

The application of the ERT technique in basic geology evolved from engineering geophysics – a branch of near-surface geophysics applied for geotechnical, civil engineering and construction issues. The method found its way to applications in imaging geological structures and its usefulness in this field is well proven, especially for fault detecting and characterisation (e.g., Colella *et al.* 2004; Diaferia *et al.* 2006; Terrizzano *et al.* 2010, 2012; Pánek *et al.* 2011). An exhaustive discussion of different aspects of the ERT method such as DC measurement theory, field acquisitions and processing can be found elsewhere (e.g., Dahlin 1996; Loke and Barker 1996; Loke 2001). The direct outcome of the ERT technique is a detailed section showing distribution of the rock medium resistivity – the value that depends on rock lithology (including mineral composition, porosity, grain size, etc.) and the presence and salinity of fluids in the pore space. Identification and outlining of the fault zones are possible by two main phenomena – the occurrence of differing lithologies on the opposite walls of the fault, resulting in contrasting zones of resistivity values, contacting across sharp boundaries, and the occurrence of fissured rocks, fault gauges, micro-karst residua and smearing of fine-grained sediments

(mineral particles) within the fault zones resulting in a drop in resistivity along the fault zone itself.

ERT measurements with 5 m electrode spacing and active measurement length up to 400 m were performed in the current study. Measurement of sections longer than 400 m would require a roll-along technique. The selected setting allowed us to image fairly compact geological objects with a penetration depth reaching 100 m. A dipole-dipole array was used due to its dense point coverage and high lateral sensitivity.
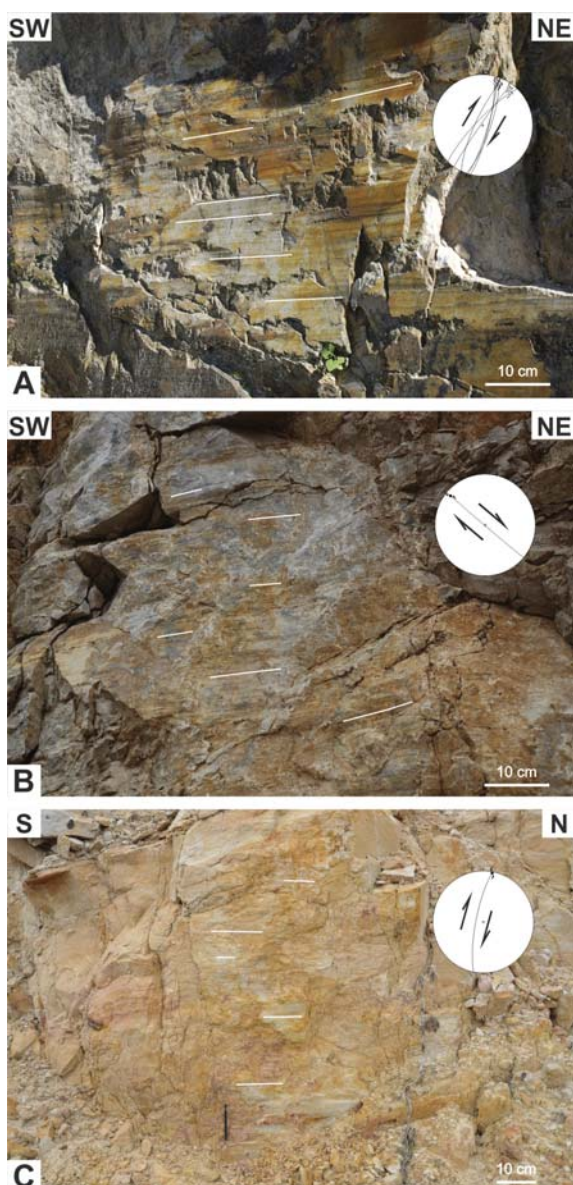
Text-fig. 5. A-C Examples of slickensides of dextral strike-slip faults. A – Slickenside of a second-order dextral strike-slip fault R in the Piaski Quarry (site No. 1). B – Slickenside of the main dextral strike-slip fault in the Gnieździska (Maćkowa Góra) Quarry (site No. 2). C – Slickenside of a second-order dextral strike-slip fault R in the Rytlów Quarry (site No. 3). For location see Text-fig. 2b

Low ambient electromagnetic noise did not cause interference with the noise-sensitive dipole-dipole array. Measurement data files were processed with Res2Dinv software, and presented as resistivity sections followed by a geological interpretation.

MNIN RESTRAINING STEPOVER

Major NW-SE and NNW-SSE-striking faults forming a complex fault pattern to the west and north-west of the HCFB are faults included in the Przedbórz-Mieczyn Fault System, and the Snochowice, Radoszyce and Diabla Góra faults belonging to the Radoszyce Fault System (Text-figs 1a and 2). The Radoszyce Fault System links with the Holy Cross Fault, the major fault in the HCFB, whereas the Straszów Fault probably connects with the Northern Łysogóry Fault (Czarnocki 1938; Jurkiewiczowa 1961; Mastella and Mizerski 2002; Konon 2007, 2015). The Snochowice Fault links in its southern part with the Mieczyn Fault and with the Gnieździska-Brzeziny and Tokarnia faults (Text-figs 1, 2). The Mieczyn Fault belonging to the Przedbórz-Mieczyn Fault System links in its southern part with the Snochowice Fault. The faults dissect Triassic, Jurassic and Cretaceous rocks characterized by different strengths.

The fault surfaces dissect Mesozoic strata, and contact at larger depths with the Palaeozoic basement formed by rocks of the HCFB (Text-fig. 4) (e.g., Czarnocki 1938, 1961; Jurkiewiczowa 1961; Jurkiewicz 1965; Filonowicz 1967; Jurkiewicz 1967; Hakenberg 1973; Filonowicz and Lindner 1986; Mastella and Konon 2002; Konon 2007). Strong differences in the strengths of the individual rocks have resulted in the formation of an anastomosing fault pattern (Text-fig. 1). Due to the curved traces, the faults merge and diverge along their strikes. Locally, the fault zones include also subparallel faults. The fault traces refract strongly at the contact between the HCFB and the Permo-Mesozoic strata (Text-fig. 1). The strike of the fault traces changes in the range of 50° of strike. The non-planar geometry of the fault planes facilitates the development of different contractional and extensional structures along the faults, such as releasing or restraining bends (e.g., Woodcock and Schubert 1994). This relationship is manifested in the Permo-Mesozoic strata by the formation of numerous bends, for example along the Gnieździska-Brzeziny Fault (Konon and Mastella 2001; Mastella and Konon 2002), and the Tokarnia, Snochowice and Mieczyn faults (Konon 2015).

In the study area, some of the fault zones consist of segments, the presence of which facilitated the for-
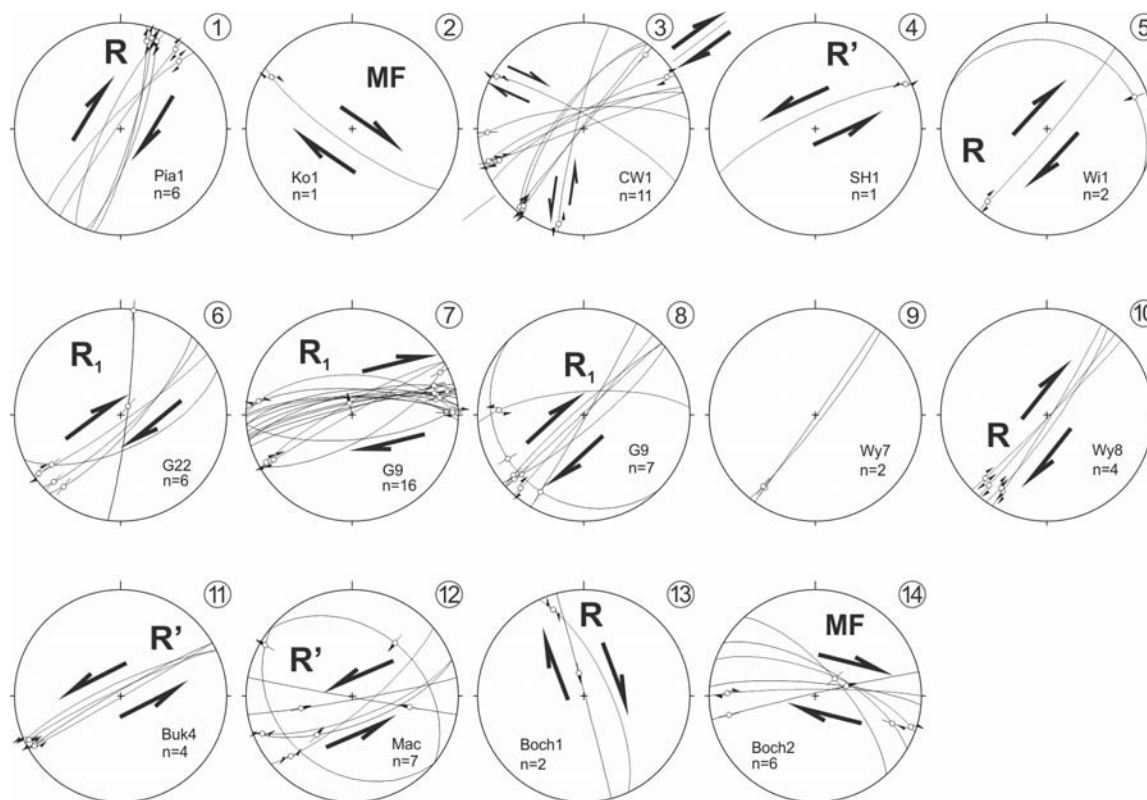
Text-fig. 6. Diagrams displaying selected dip-slip and strike-slip fault planes in the study area. MF – main fault, R, R', R$_1$ – slickensides of second-order minor faults. See text for explanations

mation of overlaps of the ends of fault traces termed as stepovers, such as the Mnin restraining stepover (Text-figs 1-4). The Mnin stepover is one of the largest contractional structures within the Permo–Mesozoic succession (Konon *et al*. 2013, 2014; Konon 2015). The stepover formed at the overlap between the NNW-SSE-trending Mieczyn Fault linked with the Przedbórz Fault and the Snochowice Fault (*op. cit.*). The structure is c. 9 km wide and c. 27 km long (Text-figs 2 and 10). Several map-scale folds formed within the stepover. In the central part of the stepover, near Mnin town, the fold axes are W–E-trending, whereas at the northern and southern ends of the stepover, they are subparallel to the surfaces of the Mieczyn and Snochowice faults (Text-fig. 2). The deflection of the fold axes suggests that the folds have a helicoidal geometry of their axial surfaces. This strong change of the fold trend suggests that the folds might have undergone modifications as a result of fault-associated dragging. Dragging of the beds resulted from the occurrence of a dextral strike-slip component along the main strike-slip faults bordering the stepover. The strike-slip component of movement along the main faults is also confirmed by field observations of slickensides (Text-figs 5, 6).

Shallow damage zones of strike-slip faults in the area adjacent to the Mnin stepover

Damage within large strike-slip fault zones mainly depends on their geometry and the material properties of the dissected rocks. Analysis based on seismic profiles (e.g., Krzywiec 2002, 2007; Woodcock and Rickards 2003) and numerical simulations performed for complex segmented structures documents the formation of flower structures at shallow depths and highly localized damage zones at larger depths (e.g., Finzi *et al*. 2009). Strain concentrates mainly along the fault cores of major fault zones. The analysis of the strike-slip fault zones dissecting the Permo-Mesozoic strata reveals that the fault cores consist of numerous slip surfaces and that the fault rocks are represented by breccias, gouges and cataclasites (Text-fig. 7).

Strike-slip fault zones display two main units: the fault core and the damage zone, which is typical of fault zones (Chester and Logan 1986; Caine *et al*. 1996, Billi *et al*. 2003; Faulkner *et al*. 2010). Detailed field mapping across the fault zones within the Permo-Mesozoic strata shows their variable width, from a few metres to several tens of metres, limited by the size of
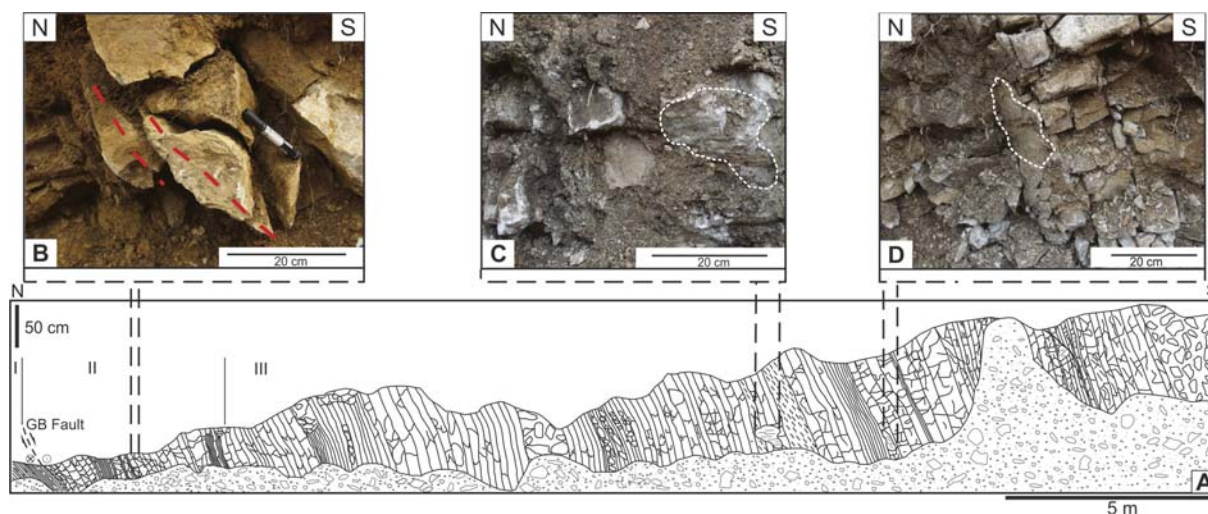
Text-fig. 7. Details of the Gnieździska-Brzeziny Fault Zone revealed in the trench in Miedzianka (after Krauze 2015, modified): A – Sketch of the fault zone: from the north incompetent Triassic claystones (I), competent thin-bedded Callovian gaizes (II), and thin- and medium-bedded Oxfordian limestones (III). B – Effects of damage of gaize beds: lens-shaped fragments of beds common within the fault zone. C, D – Examples of slickensides from subsidiary strike-slip faults cutting strongly fragmented limestones

the exposures (Text-figs 7–9). The shallow damage zones display complex structural patterns comprising subsidiary faults and fractures at different scales generated during their multistage evolution. Damage covers a relatively wide part of the fault zones that reaches up to at least 100 m (Text-figs 8 and 9). The geometry of the faults defines the failure of rocks observed e.g., along the Gnieździska-Brzeziny Fault: strong lithologies within the restraining bands resulting in broad damage zones with numerous subsidiary faults and fractures, and weaker lithologies within the releasing bends with less common fracturing (Mastella and Konon 2002; Konon 2015; Rybak-Ostrowska *et al*. 2015, 2016).

The results of failure vary along the major and subsidiary faults and depend on the location of tip-linking or wall-damage zones (e.g., Segall and Pollard 1980; Kim *et al*. 2004).

Slickensides of the major strike-slip faults are more weakly preserved in comparison with the slickensides of the subsidiary faults. Intense damage often removes the main fault planes due to significant offsets. Observations of wall- and linking-damage zones within the Permo-Mesozoic rocks reveal subsidiary faults termed as R, R' and R_1, R_1', with offsets of tens of meters and up to a few tens of centimetres wide fault zones (Text-fig. 6). The sense of movements and the shear angles (θ) indicate that the subsidiary faults R and R' represent dextral strike-slip faults and sinistral strike-slip faults, corresponding to Riedel shears, respectively (Riedel 1929). Faults R_1 and R_1'are also consistent with Riedel shears but their relation to the

major fault zones, such as the Gnieździska-Brzeziny Fault, suggests their formation in a transpression regime (e.g., Vialon 1979; Gamond and Giraud 1982; Mastella 1988; Mastella and Konon 2002).

Some of the fault zones, e.g., the Mieczyn Fault, consist of upward-diverging faults, which cut an antiformal push-up forming the Mieczyn-Lasocin Anticline (Text-figs 4 and 9). Bordering reverse faults belonging to the Mieczyn Fault Zone form a positive flower structure along this segment of the fault, indicating the presence of a contractional deformation. The reverse movement component is present in the western limb of the Mnin Syncline (Text-fig. 9). The reverse component across the fault planes suggests that both the strike-slip and the dip-slip movements occurred along the faults forming the Mnin stepover.

The effects of deformation of different rocks within the fault zones are controlled by their rock fabric and porosity. The brecciation zones mentioned above are associated both with the Middle and Upper Jurassic, and Cretaceous, limestone sequences, and reach up to several tens of metres (Text-fig. 7). The cataclastic fault rocks, typical of the Lower Jurassic sandstone sequences, show very narrow, up to a few centimetres wide, localized slip zones (Rybak-Ostrowska *et al*. 2015).

The Miocene sediments of the Carpathian Foredeep Basin mentioned above unconformably overlying the folded Mesozoic rocks as well as the Palaeozoic basement suggest that erosion could have removed 1 km or even over 2 km after the Maastrichtian and before the sedimentation of the Miocene deposits (Text-fig. 3) (Czarnocki 1938).
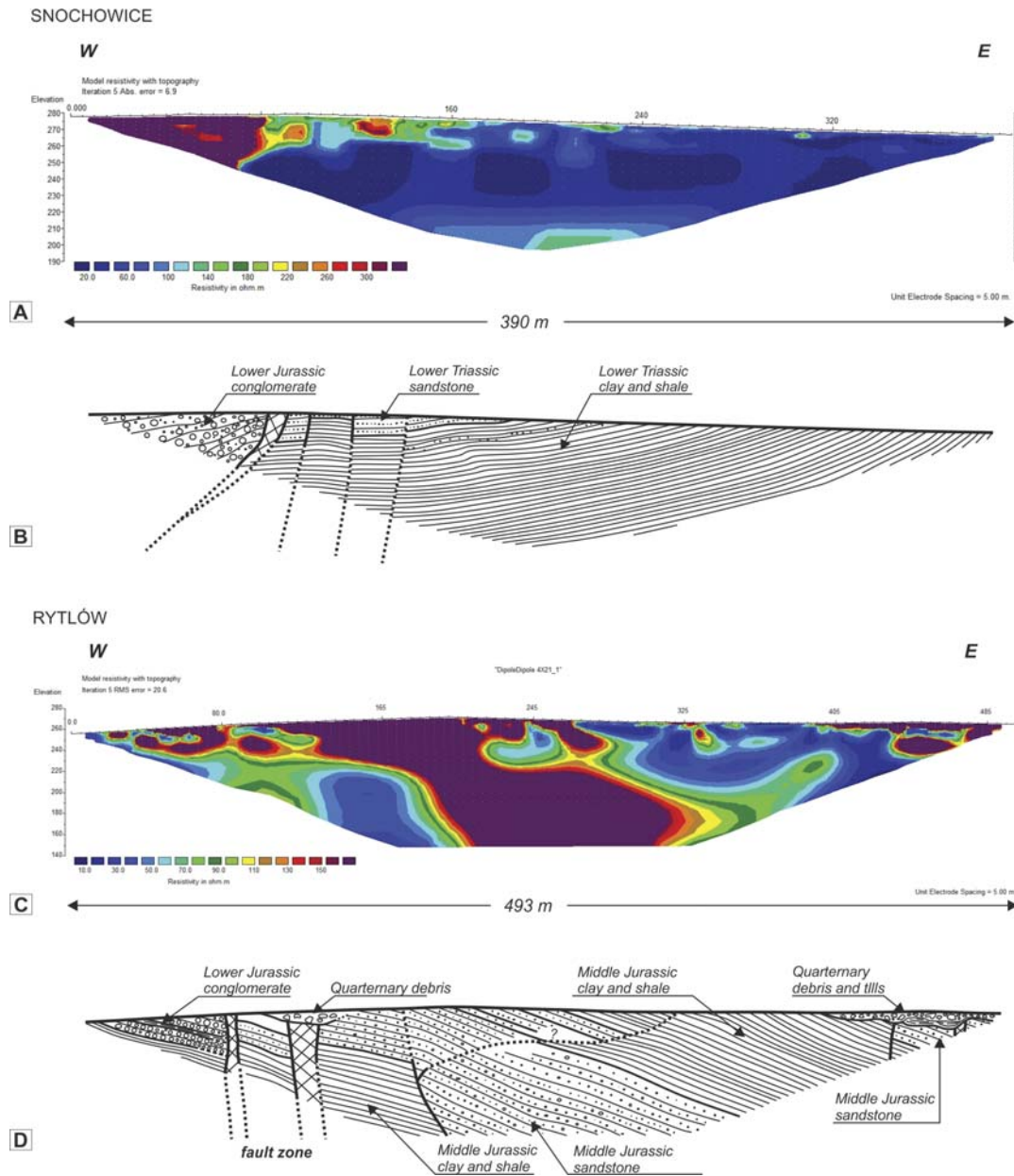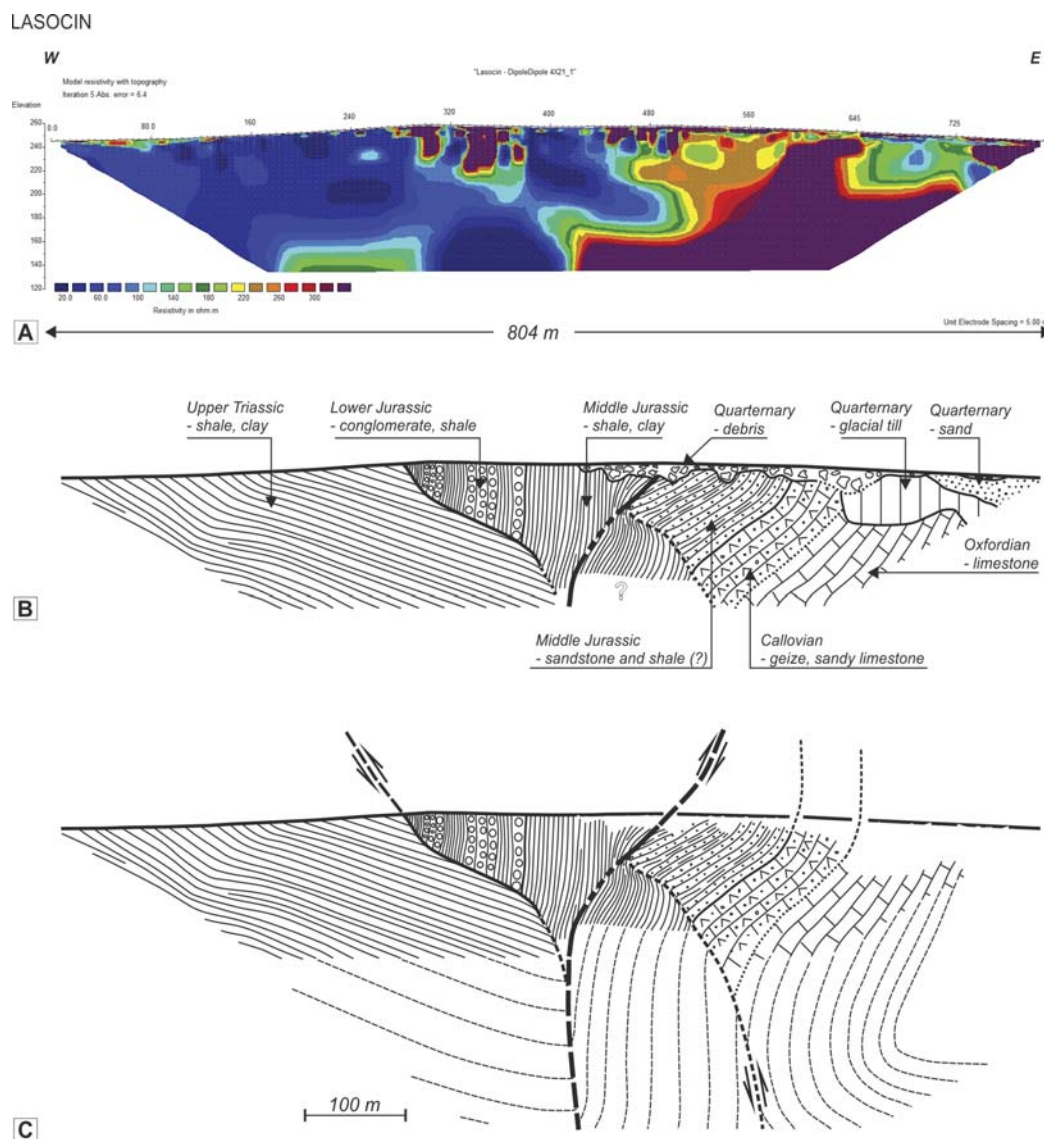
Text-fig. 8. Electrical resistivity tomography section (top) and geological interpretation (bottom) across the Snochowice Fault (A-B – section No. 1) and Mieczyn Fault (C-D – section No. 2). Dipole-dipole array, electrode spacing 5 m. For location see Text-fig. 2b

Due to this fact, it is possible to observe exhumed damage zones within the Permo-Mesozoic cover. The major dextral strike-slip fault zones show a mostly asymmetric structural pattern of damage zones recognizable in near-surface crustal conditions, in the top 1-2 km of the fault zones (Text-figs 7–9). The asymmetric pattern within the exhumed damage zones to the west of the HCFB is controlled by the non-planar geometry of the faults and the juxtaposition of strongly differing sedimentary rocks, such as incompetent Tri-

assic claystones and competent Jurassic siliciclastic and carbonate rocks with damage concentrated predominantly within the competent rocks.

DISCUSSION AND CONCLUSIONS

The fault pattern consisting of dextral strike-slip faults, recognized within the Permo-Mesozoic cover, west of the exhumed HCFB, demonstrates the signif-

Text-fig. 9. Electrical resistivity tomography section (top) and geological interpretation (bottom) across the Lasocin Fault (A-C – section No. 3). Dipole-dipole array, electrode spacing 5 m. For location see Text-fig. 2b

icant role of strike-slip faulting along the western border of the Teisseyre-Tornquist Zone, in the foreland of the Polish part of the Carpathian Orogen in the western Peri-Tethyan domain (e.g., Ziegler 1982, 1990a, b; Stampfli *et al*. 2001).

Horizontal stress was responsible for the formation of strike-slip faults, folds, contractional faults or 'pop-up structures' and 'flower structures' (e.g., Jaroszewski 1972; Kutek and Głazek 1972; Krzywiec 1999, 2001, 2002, 2007; Konon and Mastella 2001; Mastella and Konon 2002; Krzywiec *et al*. 2005; Świdrowska 2007; Zuchiewicz *et al*. 2007; Świdrowska *et al*. 2008; Jarosiński *et al*. 2009; Konon 2015).

One of these structures is the large-scale Mnin restraining stepover included in the fault pattern, formed within the Permo-Mesozoic cover, where significant refraction of the strikes of the fault traces (about 50°) is present. The refraction probably resulted from the propagation of faults through rocks of different strengths within the HCFB and its Permo-Mesozoic cover (e.g., Czarnocki 1938; Konon 2007, 2015). The change of the strikes suggests the possibility of limited reactivation of the fault zones of the HCFB. The refraction of the faults dissecting the Permo-Mesozoic rocks, to the west and south of the HCFB, is likely related also to the interaction of the two fault systems:
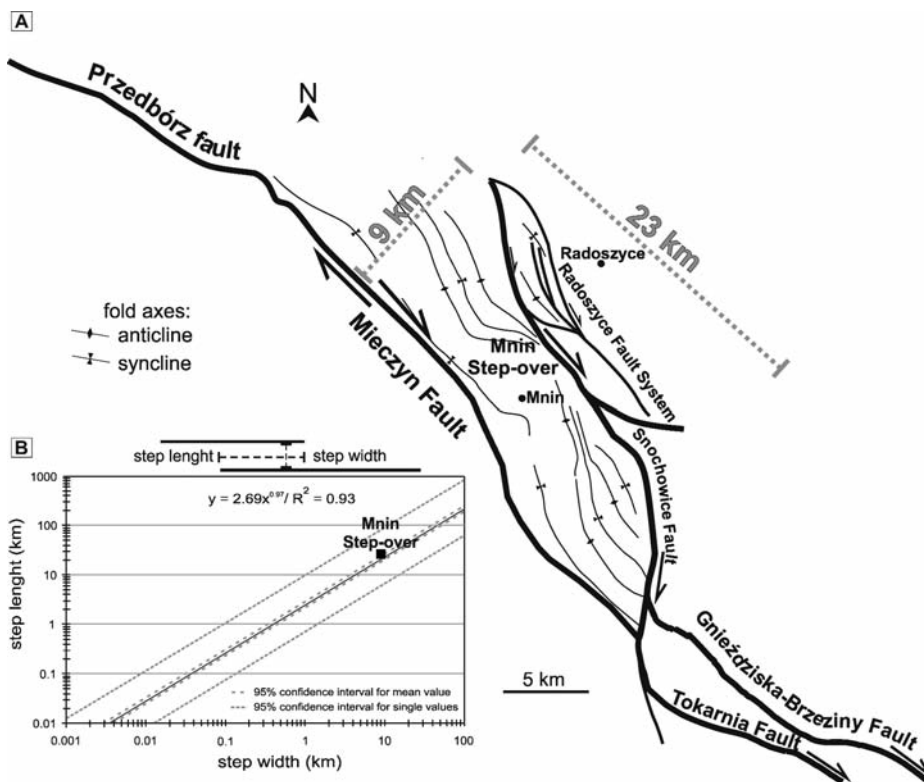
Text-fig. 10. A - Simplified tectonic sketch of the Mnin stepover with step length and width marked. B – Theoretical relationship between step width and step length of the Mnin stepover (based on de Joussineau and Aydin 2009, modified)
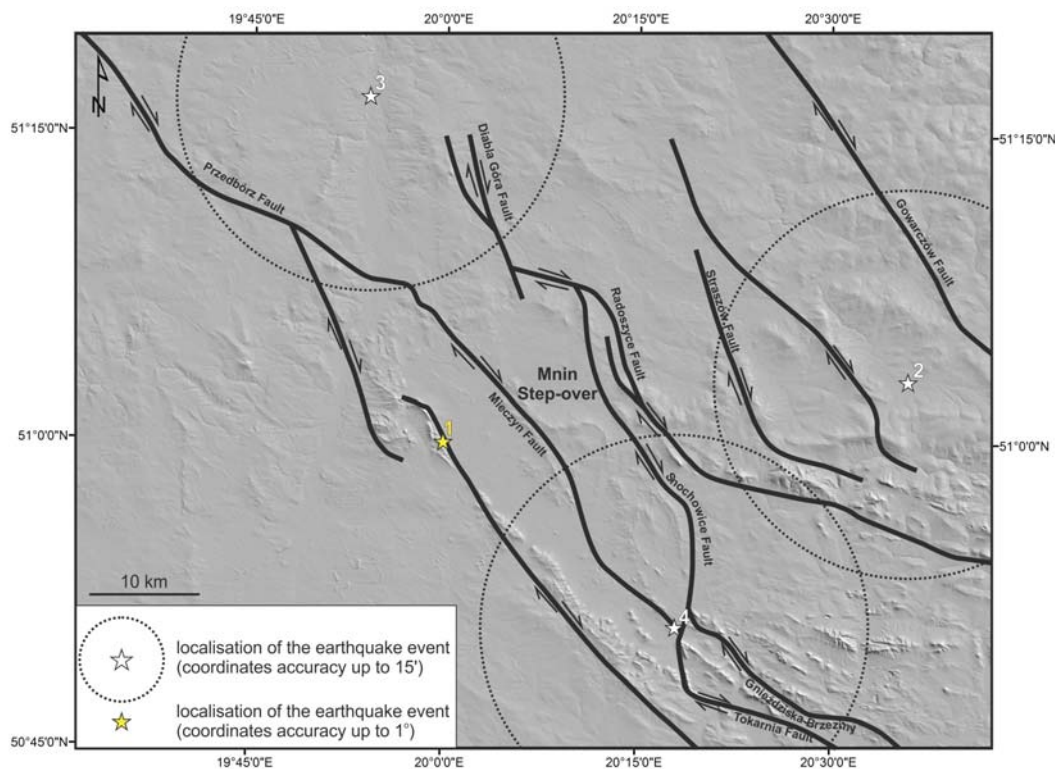
Text-fig. 11. Simplified tectonic sketch-map of the western part of the Holy Cross Mountains area with location of epicentres of earthquakes (based on: Shebalin *et al.* 1998; Guterch 2015) projected on a shaded-relief Shuttle Radar Topography Mission (SRTM) image. See text and Table 1 for explanations

www.czasopisma.pan.pl

PAN
POLSKA AKADEMIA NAUK

www.journals.pan.pl

RESTRAINING STEPOVER ALONG THE TEISSEYRE-TORNQUIST ZONE

441

NW-SE-striking faults forming probably the western border of the Teisseyre-Tornquist Zone, and WNW-ENE-striking faults belonging to the fault system of the northern margin of the Tethys Ocean (Matyja 2009).

Such a large-scale restraining stepover has so far not been described from Poland, although similar structures have been widely recognized all over the world (e.g., Sylvester 1988; Wakabayashi *et al.* 2004;
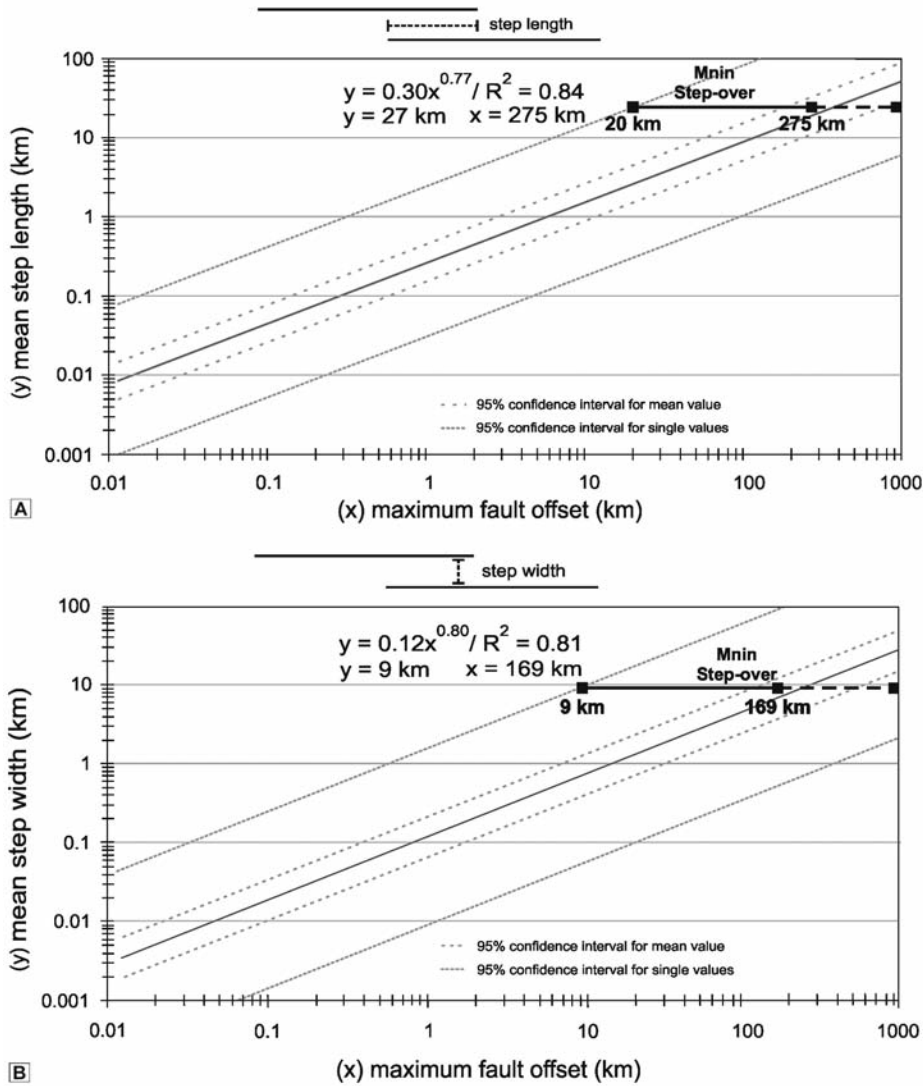
Text-fig. 12. A – Theoretical relationships between the maximum fault offset and the mean step length for strike-slip faults with the Mnin stepover parameters marked (based on de Joussineau and Aydin 2009, modified). B – Theoretical relationships between the maximum fault offset and the mean step width for strike-slip faults with the Mnin stepover parameters marked (based on de Joussineau and Aydin 2009, modified)

No.	Type of event	Data	Latitude (Y)	Longitude (X)	Source quality	coordinates accuracy	Intensity
1*	n/a	08.08.1303	51.0	20.0	n/a	(X, Y) +/- 1 degree	6 (+/- 1.5) (based on MSK-64 scale)
2**	n/a	05.02.1837	50.68	21.04	reliable sources data	6' < (X, Y) < 15'	6 (+/- 1) (based on EMS-98 scale)
3**	main event	20.11.1926	51.28	19.90	reliable sources data	6' < (X, Y) < 15'	6 (+/- 1) (based on EMS-98 scale)
4**	earthquake swarm	06.02.1932	50.6	21.2	reliable sources data	6' < (X, Y) < 15'	6 (+/- 1) (based on EMS-98 scale)

* - based on Shebalin *et al* (1998); ** - based on Guterch (2015)
Intensity scales: EMS-98 (European Macroseismic Scale); MSK-64 (Medvedev–Sponheuer–Karnik scale).

Table 1. Historical earthquake epicentres in the Holy Cross Mountains region based on Shebalin *et al.* (1998) and Guterch (2015). Location of seismic events in Text-fig. 11

Wakabayashi 2007; Morley *et al.* 2009; Babaahmadi *et al.* 2010; Nadimi and Konon 2012).

Stepovers associated with strike-slip faulting, where the folds are modified in a contractional overlap of faults, and the length-to-width ratios range from 2.5 to 3, were described e.g., along the San Andreas Fault (Sylvester 1988; Wakabayashi *et al.* 2004; Wakabayashi 2007), along the northern margin of the Sanandaj-Sirjan Zone in the Zagros Orogen (Morley *et al.* 2009; Babaahmadi *et al.* 2010), and in the central part of this zone (Nadimi and Konon 2012).

Significant offsets facilitate the migration of stepovers as in the case of the active Mount Diablo restraining stepover (Wakabayashi 1999, 2007; Wakabayashi *et al.* 2004). The active Mount Diablo fold-and-thrust belt, whose strike is oblique to the boundary faults, formed within the stepover. The mean step length of the Mount Diablo stepover is c. 30 km. The total late Cenozoic dextral slip that has been transferred through the Mount Diablo stepover is at least 18 km, whereas the total displacement along the eastern faults of the San Andreas Fault System is about 230–250 km (Wakabayashi 2007). According to Wakabayashi (1999), individual structures associated with strike-slip faulting, such as restraining stepovers, slip transfers, or bends have accommodated tens of kilometres of slip along the San Andreas Fault System.

Another example of active fault stepovers affecting the initiation of earthquakes is the overlap between the Indes and Qom faults and the Zefreh and Nain-Dehshir Faults forming *en échelon* arrays, where restraining stepover zones were recognized (Morley *et al.* 2009; Babaahmadi *et al.* 2010). The estimated total offsets along the Indes and the Qom-Zefreh faults are approximately 40-50 km (Allen *et al.* 2011).

Similar active restraining stepovers as e.g., the Hasan Robat, Pars and Najafabad restraining stepovers formed along the longitudinal fault systems to the south of the Indes and Qom Faults in the central part of the Sanandaj-Sirjan zone (SSZ). The tectonic block was horizontally sheared in a manner consistent with the simple shear 'card-deck model' (Nadimi and Konon 2012). The mean step lengths of the Hasan Robat, Pars and Najafabad stepovers are c. 50, 15 and 30 km, respectively. In the left-stepping stepover zone, between the segments of the major faults, developed map-scale folds with a helicoidal geometry of the axial surfaces. A similar restraining stepover, in which the folds have a helicoidal geometry of the axial surfaces, formed between the left stepping segments of the major faults near Najafabad.

These examples show that large restraining stepovers with the mean step lengths over 20-30 km form when the offsets along the strike-slip faults exceed at least 10 km. This suggests that the displacements along the strike-slip faults in the study area might be also significant. Most of the strike-slip faults dissecting the Permo-Mesozoic strata, which were recognized to the west of the HCFB are longitudinal, and the magnitudes of displacements along the faults are difficult to estimate due to the lack of clearly determined markers, such as e.g., the offset of Holocene deposits, rivers, streams or other geological structures. One example of the measured strike-separation of the Oxfordian-Kimmeridgian limestones comes from the southern limb of the Bolmin Syncline, where Jurassic rocks are dextrally offset by the Tokarnia Fault by about 2 km (Text-fig. 2c).

The area of Poland displays a generally low-magnitude seismicity (e.g., Shebalin *et al.* 1998; Guterch 2009, 2015). Epicentres of seismic events are located mostly in the Western Carpathians, in the Sudetes and along the Teisseyre-Tornquist Zone showing the activity of the fault zones. A few historical earthquakes with an estimated epicentral intensity I_O=5-6 in the EMS-98 and MSK-64 scales occurred in the vicinity of the investigated faults near the Holy Cross Mountains (*op. cit.*) (Text-fig. 11, Table 1). Low-magnitude seismicity limits the identification of geomorphic evidence for active strike-slip faulting.

For estimation of the magnitudes of maximum displacements along strike-slip faults based on the stepover parameters, it is necessary to consider the theoretical relationships between the maximum fault offsets/mean step length, as well as between the maximum fault offsets/mean step width according to the laws of de Joussineau and Aydin (2009). In the case of the Snochowice and Mieczyn faults, the Mnin stepover is the only structure available for measurements. This causes significant uncertainty in the estimation of the displacement.

The step length and mean step width of the Mnin stepover are c. 27 km and 9 km, respectively (Text-fig. 10). The length-to-width ratio equal to 3, calculated for the Mnin stepover demonstrates an almost best fit to the quasi-linear positive power law relationship: $y = 2.69x^{0.97}/R^2 = 0.93$ (de Joussineau and Aydin 2009). This puts the Mnin stepover close to the most typical structures of this type.

The estimated value of the maximum offset along the Snochowice and Mieczyn Fault System, calculated based on the relationships between the step length/maximum fault offset as well as the mean step width/maximum fault offset, ranges between 9–20 km and 169–275 km (Text-fig. 12). Only the lower values

of the estimated range seems to fit into the tectonic setting of the area. Significant values of the length and width of the stepover suggest that the Snochowice and Mieczyn faults belong to a large strike-slip fault system. The obtained results based on the present state of knowledge are difficult to prove and they indicate the need for further research.

The precise timing of the formation of the Mnin restraining stepover is difficult. The youngest folded rocks involved in the folds within the stepover are of Jurassic age. Cretaceous rocks occur to the south of the structure near Małogoszcz, within the hinges of the anticline and syncline, in a situation similar to that with the hinge of the Bolmin Syncline dissected by the Gnieździska-Brzeziny and Tokarnia Faults. Constraints on the timing of the formation of the strike-slip faults in the Permo-Mesozoic strata are provided by deflection of the fold axes within the Mnin stepover. The folds might have undergone modifications as a result of fault-associated dragging after the Cretaceous and before the Miocene, which is consistent with the observation that the folded rocks are unconformably overlain by Miocene rocks (Text-fig. 2a) (e.g., Czarnocki 1938). Consequently, the deformation might have been associated with the Cretaceous/Palaeogene inversion stage (Pożaryski 1964; Kutek and Głazek 1972, Dadlez *et al.* 1997; Krzywiec 2000, 2002, 2007; Hakenberg and Świdrowska 2001; Świdrowska 2007; Świdrowska *et al.* 2008). The lack of Palaeocene deposits (Piwocki 2004) in the study area does not allow a clear estimation of the age of the end of the inversional deformation. According to some authors (Pożaryski and Brochwicz-Lewiński 1979; Krzywiec 2006), the inversion ended in the Palaeocene or in the early Eocene (Kutek and Głazek 1972; Narkiewicz *et al.* 2010).

Strike-slip faulting during the Late Cretaceous – Palaeogene was documented along the Grójec Fault (Krzywiec 2009a), north-east of the study area (Text-fig. 1b). Similarly, strike-slip faulting during the Late Cretaceous–early Cenozoic times, was recognized south-west of the study area, along the WNW-ESE-striking Elbe Fault System (Text-fig. 1b). This fault system responded to regional compression with a significant uplift of up to 4 km (Scheck *et al.* 2002).

A younger strike-slip component on the fault planes dissecting the Cenozoic rocks was observed to the west of Przedbórz in the Kleszczów Graben (e.g., Hałuszczak *et al.* 1995; Felisiak 2001), along the margins of the Carpathian Foredeep Basin (e.g., Jarosiński 1992; Jarosiński *et al.* 2009; Lamarche *et al.* 2002), as well as to the south-east of the HCFB along the Ryszkowa Wola Horst (Krzywiec *et al.* 2005). Strike-slip activity during the Middle to Late Pleistocene caused by fault movements was also observed on NW-SE-trending reverse faults in a transpressional regime (Gotowała and Hałuszczak 2002). The observations suggest that the faults forming the fault pattern east of the Kleszczów graben, where the Mnin stepover occurs, could be reactivated during the Cenozoic or even during present-day deformation, which is suggested by earthquake analysis (e.g., Shebalin *et al.* 1998; Guterch 2009, 2015).

Acknowledgments

REFERENCES

Alexandrowicz, S.W., Garlicki, A. and Rutkowski, J. 1982. Podstawowe jednostki litostratygraficzne miocenu zapadliska przedkarpackiego. *Sprawozdania z posiedzeń naukowych Instytutu Geologicznego. Kwartalnik Geologiczny*, **26**, 470–471.

Allen, M.B., Kheirkhah, M., Emami, M.H. and Jones, S.J. 2011. Right-lateral shear across Iran and kinematic change in the Arabia–Eurasia collision zone. *Geophysical Journal International*, **184**, 555–574.

Babaahmadi A., Safaei H., Yassaghi A., Vafa H., Naeimi A., Madanipour M. and Ahmadi M. 2010. A study of Quaternary structures in the Qom region, west Central Iran. *Journal of Geodynamics*, **50**, 355–367.

Barski, M. 1999. Dinocyst stratigraphy of the Jurassic black clays from Holy Cross Mts area (Central Poland). *Przegląd Geologiczny*, **47**, 718–722. [In Polish with English summary]

Billi, A., Salvini, F. and Storti, F. 2003. The damage zone–fault core transition in carbonate rocks: implications for fault growth structure and permeability. *Journal of Structural Geology*, **25**, 1779–1794.

Caine, J.S., Evans, J.P. and Forster, C.B. 1996. Fault zone architecture and permeability structure. *Geology*, **24**, 1025–1028.

Chester, F.M. and Logan, J.M. 1986. Implications for mechanical–properties of brittle faults from observations of the Punchbowl fault zone, California. *Pure and Applied Geophysics*, **124**, 79–106.

Cieśla, E. and Lindner, L. 1990. Geological Map of Poland, Końskie sheet (740), scale 1:50 000. Wydawnictwa Geologiczne; Warszawa.

Colella, A., Lapenna, V. and Rizzob, E. 2004. High-resolution imaging of the High Agri Valley Basin (Southern Italy) with electrical resistivity tomography. *Tectonophysics*, **386**, 29–40.

Czapowski, G. 2004. Zapadlisko przedkarpackie. Otoczenie Gór Świętokrzyskich. In: T. Peryt and M. Piwocki (Eds), Budowa geologiczna Polski. T.1. Stratygrafia. Część 3a – Kenozoik, Paleogen, Neogen, pp. 239–245. Wydawnictwa Geologiczne; Warszawa.

Czarnocki, J. 1938. Carte geologique generale de la Pologne, feuille 4, Kielce, Edition du Service Geologique de Pologne, scale 1:100 000.

Czarnocki, J. 1948. Przewodnik 20 Zjazdu Polskiego Towarzystwa Geologicznego w Górach Swietokrzyskich w r. 1947. *Rocznik Polskiego Towarzystwa Geologicznego*, **17**, 237–299.

Czarnocki, J. 1950. Geology of the Łysa Góra Region (Święty Krzyż Mountains) in connection with the problem of iron ores at Rudki. *Prace Państwowego Instytutu Geologicznego*, **1**, 1–404. [In Polish with English summary]

Czarnocki, J. 1956. Surowce mineralne w Górach Świętokrzyskich. *Prace Geologiczne Instytutu Geologicznego*, **12a**, 5–108.

Czarnocki, J. 1961. Materiały do przeglądowej mapy geologicznej Polski. Region Świętokrzyski. Arkusz Kielce. Wyd. B zaktualizowane, skala 1:100 000. Wydawnictwa Geologiczne; Warszawa.

Dadlez, R. 1994. Strike-slip movements in the Polish Lowlands. *Geological Quarterly*, **38**, 307–318.

Dadlez, R. 1997. Epicontinental basins in Poland: Devonian to Cretaceous-relationship between the crystalline basement and sedimentary infill. *Geological Quarterly*, **41**, 419–432.

Dadlez, R. 2003. Mesozoic thickness pattern in the Mid–Polish Trough. *Geological Quarterly*, **47**, 223–240.

Dadlez, R. 2006. The Polish Basin – relationship between the crystalline, consolidated and sedimentary crust. *Geological Quarterly*, **50**, 43–58.

Dadlez, R., Narkiewicz, M., Stephenson, R.A. Visser M.T.M. and Van Wees J.-D. 1995. Tectonic evolution of the Mid-Polish Trough: modelling implications and significance for central European geology. *Tectonophysics*, **252**, 179–195.

Dadlez, R., Jóźwiak, W. and Młynarski, S. 1997. Subsidence and inversion in the western part of Polish basin – data from seismic velocities. *Geological Quarterly*, **41**, 197–208.

Dahlin, T. 1996. 2D resistivity surveying for environmental and engineering applications. *First Break*, **14**, 275–283.

de Joussineau, G. and Aydin, A. 2009. Segmentation along Strike–Slip Faults Revisited. *Pure Applied Geophysics*, **166**, 1575–1594.

Diaferia, I., Barchi, M., Loddo, M., Schiavone, D. and Sinis-calchi, A. 2006. Detailed imaging of tectonic structures by multiscale Earth resistivity tomographies: The Colfiorito normal faults (central Italy). *Geophysical Research Letters*, **33**, 1–4.

Faulkner, D.R., Jackson, C.A.L., Lunn, R.J., Schlische, R.W., Shipton, Z.K., Wibberley, C.A.J. and Withjack, M.O. 2010. A review of recent developments concerning the structure, mechanics and fluid flow properties of fault zones. *Journal of Structural Geology*, **32**, 1557–1575.

Felisiak, I. 2001. Południowy uskok główny rowu Kleszczowa – koncepcja a rzeczywistość. *Przegląd Geologiczny*, **49**, 307–311.

Filonowicz, P. 1967. Geological Map of Poland, Morawica sheet (814), scale 1:50 000. Wydawnictwa Geologiczne; Warszawa.

Filonowicz, P. 1968. Explanations to Geological Map of Poland, Morawica sheet (814), scale 1:50 000. Wydawnictwa Geologiczne; Warszawa.

Filonowicz, P. and Lindner, L. 1986. Geological Map of Poland, Piekoszów sheet (851), scale 1:50 000. Wydawnictwa Geologiczne; Warszawa.

Finzi, Y., Hearn, E.H., Ben–Zion, Y. and Lyakhovsky, V. 2009. Structural properties and deformation patterns of evolving strike–slip faults: Numerical simulations incorporating damage rheology. *Pure and Applied Geophysics*, **166**, 1537–1573.

Gamond, J.F. and Giraud, A. 1982. Identification des zones de faille a l'aide des associations de fractures de second ordre. *Bulletin de la Société Géologique de France*, **24**, 755–762.

Giżejewska, M. 1975. Jura środkowa niecki miechowskiej i południowo–zachodniego obrzeżenia Gór Świętokrzyskich. *Przegląd Geologiczny*, **11**, 530–535.

Golonka, J., Oszczypko, N. and Ślączka, A. 2000. Late Carboniferous–Neogene geodynamic evolution and palaeogeography of the circum–Carpathian region and adjacent areas. *Annales Societatis Geologorum Poloniae*, **70**, 107–136.

Gotowała, R. and Hałuszczak, A. 2002. The Late Alpine structural development of the Kleszczów Graben (Central Poland) as a result of a reactivation of the pre–existing, regional dislocations. *EGU Stephan Mueller Special Publication Series*, **1**, 137–150.

Grzybowski, K. and Kutek, J. 1967. Geological Map of Poland, Lubień sheet (738), scale 1:50 000. Wydawnictwa Geologiczne; Warszawa.

Guterch, B. 2009. Seismicity in Poland in the light of historical records. *Przegląd Geologiczny*, **57**, 513–520.

Guterch, B. 2015. Seismicity in Poland: Updated Seismic Catalog. In: B. Guterch and J. Kozák (Eds), Studies of Historical Earthquakes in Southern Poland, Outer Western Carpathian Earthquake of December 3, 1786, and First Macroseismic Maps in 1858–1901: 75–101. Springer International Publishing AG Switzerland.

Gutowski, J. and Koyi, H.A. 2007. Influence of oblique basement strike–slip faults on the Mesozoic evolution of the south-eastern segment of the Mid-Polish Trough. *Basin Research*, **19**, 67–86.

Hałuszczak, A., Gotowała, R. and Czarnecki, L. 1995. Uskok Folwarku – przejawy tektoniki przesuwczej w zachodniej części odkrywki Bełchatów. *Przegląd Geologiczny*, **43**, 9–11.

Hakenberg, M. 1973. Geological Map of Poland, Chęciny sheet (850), scale 1:50 000. Wydawnictwa Geologiczne; Warszawa.

Hakenberg, M. 1974. Explanations to Geological Map of Poland, Chęciny sheet (850), scale 1:50 000. Wydawnictwa Geologiczne; Warszawa.

Hakenberg, M. 1978. Albian – Cenomanian palaeotectonics and palaeogeography of the Miechów Depression, northern part. *Studia Geologica Polonica*, **58**, 5–104. [In Polish with English summary]

Hakenberg, M., Kutek, J., Matyja, B.A., Mizerski, W., Rutkowski, J., Stupnicka, E., Świdrowska, J. and Trammer, J. 1976. Stratygrafia, wykształcenie litologiczne i tektonika mezozoiku południowo–zachodniego obrzeżenia Gor Świętokrzyskich. In: W. Pożaryski (Ed.), Przewodnik 47 Zjazdu Polskiego Towarzystwa Geologicznego, pp. 185–202. Warszawa.

Hakenberg, M. and Świdrowska, J. 2001. Cretaceous basin evolution in the Lublin area along the Teisseyre–Tornquist Zone (SE Poland). *Annales Societatis Geologorum Poloniae*, **71**, 1–20.

Jamison, W.R. 1991. Kinematics of compressional fold development in convergent wrench terranes. *Tectonophysics*, **190**, 209–232.

Janiec, J. 1991. Geological Map of Poland, Żarnów sheet (739), scale 1:50 000. Wydawnictwa Geologiczne; Warszawa.

Jarosiński, M. 1992. The tectonics of the argillaceous rocks of the cover of the sulfhur deposit in Machów near Tarnobrzeg in the light of the mesostructural analysis. *Geological Quarterly*, **36**, 121–150. [In Polish with English summary]

Jarosiński, M., Poprawa, P. and Ziegler, P.A. 2009. Cenozoic dynamic evolution of the Polish Platform. *Geological Quarterly*, **53**, 3–26.

Jaroszewski, W. 1972. Mesoscopic structural criteria of tectonics of non–orogenic areas: an example from the north–eastern Mesozoic margin of the Świętokrzyskie Mountains. *Studia Geologica Polonica*, **37**, 9–210.

Jaroszewski, 1973. Analiza tektonicznych pól naprężeń jako kryterium poszukiwawcze. *Przegląd Geologiczny*, **21**, 523–528.

Jaroszewski, W. 1980. Tektonika uskoków i fałdów, pp. 1–360. Wydawnictwo Geologiczne; Warszawa.

Jurkiewicz, I. 1965. Geological Map of Poland, Czermno sheet (776), scale 1:50 000. Wydawnictwa Geologiczne; Warszawa.

Jurkiewicz, I. 1967. Geological Map of Poland, Radoszyce sheet (777), scale 1:50 000. Wydawnictwa Geologiczne; Warszawa.

Jurkiewicz, I. 1968. Explanations to Geological Map of Poland, Czermno sheet (776), scale 1:50 000. Wydawnictwa Geologiczne; Warszawa.

Jurkiewiczowa, I. 1961. Materiały do przeglądowej mapy geologicznej Polski. Region Świętokrzyski. Arkusz Przedbórz. Wyd. B zaktualizowane, skala 1:100 000. Wydawnictwa Geologiczne; Warszawa.

Jurkiewiczowa, I. 1967. Lias zachodniego obrzeżenia Gór Świętokrzyskich i jego paralelizacja z liasem Wyżyny Krakowsko–Częstochowskiej. *Biuletyn Instytutu Geologicznego*, **200**, 5–90.

Kim, Y., Peacock, D.C.P. and Sanderson, D.J. 2004. Fault damage zones. *Journal of Structural Geology*, **26**, 503–517.

Konon, A. 2007. Strike–slip faulting in the Kielce unit, Holy Cross Mountain, central Poland. *Acta Geologica Polonica*, **57**, 415–441.

Konon, A. 2015. Przejawy przesuwczości w obrębie południowo–zachodniego permo–mezozoicznego obrzeżenia Gór Świętokrzyskich. In: S. Skompski and W. Mizerski (Eds), Przewodnik 84 Zjazdu Naukowego Polskiego Towarzystwa Geologicznego, pp. 59–67. Państwowy Instytut Geologiczny – PIB, Warszawa.

Konon, A. and Mastella, L. 2001. Structural evolution of the Gnieździska syncline – regional implications for the mesozoic margin of the Holy Cross Mountains (central Poland). *Annales Societatis Geologorum Poloniae*, **71**, 189–199.

Konon, A. and Śmigielski, M. 2006. DEM–based structural mapping (examples from the Holy Cross Mountains and the Polish Outer Carpathians). *Acta Geologica Polonica*, **56**, 1 –16.

Konon, A., Ludwiniak, M., Rybak–Ostrowska, B., Ostrowski, S., Śmigielski, M., Uroda, J. and Wyglądała M. 2013, A contractional stepover in the region of the Mnin Syncline formed during the inversion of the Polish Basin. In: L. Fodor and S. Kövér (Eds), CETeG 2013 – Meeting of the Central European Tectonic Studies Group, pp. 29–30. Vargesztes; Hungary.

Konon, A., Nadimi, A., Rybak–Ostrowska, B., Wyglądała, M., Śmigielski, M., Ludwiniak, M. and Uroda, J. 2014. Active contractional stepovers in strike slip fault systems – comparison of the structures from the foreland of the Polish part of the Carpathian Orogen and the Sanandaj–Sirjan Zone (Zagros Orogen, Iran). In: J. Xiaochi, U. Katsumi, Y. JR. Graciano and C. Pol (Eds), The Third International International Symposium of International Geosciences Programme Project 589 (IGCP–589) UNESCO/IUGS, "Development of the Asian Tethyan

Realm: Genesis, Process and Outcomes", pp. 117–124. Tehran; Iran.

Kowalski, W.R. 1975. Tektonika zachodniego zakończenia antykliny chęcińskiej i otaczających ja struktur obrzeżenia mezozoicznego. *Rocznik Polskiego Towarzystwa Geologicznego*, **45**, 45–61.

Krajewski, R. 1961. Materiały do przeglądowej mapy geologicznej Polski. Region Świętokrzyski. Arkusz Końskie. Wyd. B zaktualizowane, skala 1:100 000. Wydawnictwa Geologiczne; Warszawa.

Krauze, A. 2015. Petrophysical analysis of the Gnieździska–Brzeziny fault zone in the region of Miedzianka (Holy Cross Mountains) – praca dyplomowa magisterska, pp. 1–85. Uniwersytet Warszawski, Wydział Geologii; Warszawa.

Krzywiec, P. 1999. Mioceńska ewolucja tektoniczna wschodniej części zapadliska przedkarpackiego (Przemyśl–Lubaczów) w świetle interpretacji danych sejsmicznych. *Prace Państwowego Instytutu Geologicznego*, **168**, 249–276.

Krzywiec, P. 2000. O mechanizmach inwersji bruzdy środkowopolskiej – wyniki interpretacji danych sejsmicznych. *Biuletyn Państwowego Instytutu Geologicznego*, **393**, 135–166.

Krzywiec, P. 2001. Contrasting tectonic and sedimentary history of the central and eastern parts of the Polish Carpathian foredeep basin–results of seismic data interpretation. *Marine and Petroleum Geology*, **18**, 13–38.

Krzywiec, P. 2002, Mid-Polish Trought inversion – seismic examples, main mechanism, and its relatopnship to the Alpine–Carpathian collision, *EGU Stephan Mueller Special Publication Series*, **1**, 151–165.

Krzywiec, P. 2006. Structural inversion of the Pomeranian and Kuiavian segments of the Mid-Polish Trough – lateral variations in timing and structural style. *Geological Quarterly*, **51**, 151–168.

Krzywiec, P. 2007. Nowe spojrzenie na tektonikę regionu lubelskiego (SE Polska) oparte na wynikach interpretacji danych sejsmicznych. *Biuletyn Państwowego Instytutu Geologicznego*, **422**, 1–18.

Krzywiec, P. 2009a. Structure and Mesozoic-Cenozoic evolution of the Grójec strike-slip fault zone – results of seismic data interpretation. *Geologia AGH*, **35**, 377–386. [In Polish with English summary]

Krzywiec, P. 2009b. Devonian–Cretaceous repeated subsidence and uplift along the Teisseyre–Tornquist zone in SE Poland – Insight from seismic data interpretation. *Tectonophysics*, **475**, 142–159.

Krzywiec, P., Aleksandrowski, P., Ryzner-Siupik, B., Papiernik, B., Siupik, J., Mastalerz, K. and Kasiński, J. 2005. Budowa geologiczna i geneza mioceńskiego zrębu Ryszkowej Woli w rejonie Sieniawy–Rudki (wschodnia część zapadliska przedkarpackiego) – wyniki interpretacji danych sejsmiki 3D. *Przegląd Geologiczny*, **53**, 656–663.

Krzywiec, P., Gutowski, J., Walaszczyk, I., Wróbel, G. and Wybraniec, S. 2009. Tectonostratigraphic model of the Late Cretaceous inversion along the Nowe Miasto–Zawichost Fault Zone, SE Mid-Polish Trough. *Geological Quarterly*, **53**, 27–48.

Kuleta, M. and Zbroja, S. 2006. Wczesny etap rozwoju pokrywy permsko–mezozoicznej w Górach Świętokrzyskich. In: S. Skompski and A. Żylińska (Eds), 77 Zjazd Naukowy Polskiego Towarzystwa Geologicznego, Ameliówka k. Kielc, 28–30 czerwca 2006r., materiały konferencyjne, pp. 105–125. Warszawa.

Kutek, J. 1968. The Kimmeridgian and Uppermost Oxfordian in the SW margin of the Holy Cross Mts, Central Poland. Part I, Stratigraphy. *Acta Geologica Polonica*, **18**, 493–586. [In Polish with English summary]

Kutek, J. 2001. The Polish Permo-Mesozoic Rift Basin. In: P.A. Ziegler, W. Cavazza, A.H.F. Robertson and S. Crasquin-Soleau (Eds), Peri-Tethys Memoir 6: Peri-Tethyan Rift/Wrench Basins and Passive Margins. *Memoires Du Museum National d'histoire Naturelle*, **186**, 213–236.

Kutek, J. and Głazek, J. 1972. The Holy Cross area, Central Poland, in the Alpine cycle. *Acta Geologica Polonica*, **22**, 603–653.

Kwapisz, B. 1983. Geological Map of Poland, Secemin sheet (848), scale 1:50 000. Wydawnictwa Geologiczne; Warszawa.

Lamarche, J., Bergerat, F., Lewandowski, M., Mansy, J.L., Świdrowska, J. and Wieczorek, J. 2002. Variscan to Alpine heterogeneous palaeo-stress field above a major Palaeozoic suture in the Carpathian foreland (southeastern Poland). *Tectonophysics*, **357**, 55–80.

Loke, M.H. 2001. Electrical imaging surveys for environmental and engineering studies. A Practical Guide to 2-D and 3-D Surveys: RES2DINV Manual, 1–65. Available at www.geoelectrical.com.

Loke, M.H. and Barker, R.D. 1996. Rapid least squares inversion of apparent resistivity pseudosections by a quasi–Newton method. *Geophysical Prospecting*, **44**, 131–152.

Mandl, G. 1987. Tectonic deformation by rotating parallel faults: the "bookshelf" mechanism. *Tectonophysics*, **141**, 277–316.

Marcinowski, R. and Radwański, A. 1983. The Mid-Cretaceous transgression onto the Central Polish Uplands (marginal part of the Central European Basin). *Zitteliana*, **10**, 65–95.

Mastella, L. 1988. Budowa i ewolucja strukturalna okna tektonicznego Mszany Dolnej, polskie Karpaty zewnętrzne. *Annales Societatis Geologorum Poloniae*, **58**, 53–173.

Mastella, L. and Konon, A. 2002. Non–planar strike–slip Gnieździska–Brzeziny fault (SW Mesozoic margin of the Holy Cross Mountains, central Poland). *Acta Geologica Polonica*, **52**, 471–480.

Mastella, L. and Mizerski, W. 2002. Budowa geologiczna jednostki łysogórskiej (Góry Świętokrzyskie) na podstawie analizy zdjęć radarowych. *Przegląd Geologiczny*, **50**, 767–772.

Matyja, B.A. 1977. The Oxfordian in the south-western margin of the Holy Cross Mts. *Acta Geologica Polonica*, **27**, 41–64.

Matyja, B.A. 2009. Development of the Mid–Polish Trough versus Late Jurassic evolution in the Carpathian Foredeep area. *Geological Quarterly*, **53**, 49–62.

Matyja, B.A. 2012. Mezozoik. In: S. Skompski (Ed.), Góry Świętokrzyskie. 25 najważniejszych odsłonięć geologicznych. Uniwersytet Warszawski, Wydział Geologii, 17–23. Warszawa.

Matyja, B.A., Wierzbowski, A. and Drewniak, A. 1996. Węglanowe osady basenu późnojurajskiego zachodniego obrzeżenia Gór Świętokrzyskich. In: P.H. Karnkowski (Ed.), Analiza basenów sedymentacyjnych a nowoczesna sedymentologia. Materiały konferencyjne V Krajowego Spotkania Sedymentologicznego, A1–16. Warszawa.

Mazur, S., Krzywiec, P. and Scheck–Wenderoth, M. 2005. Different modes of Late Cretaceous–Early Tertiary inversion in the Noth German and Polish Basin. *International Journal of Earth Sciences* (*Geologische Rundschau*), **94**, 782–798.

McClay, K. and Bonora, M. 2001. Analog models of restraining stepovers in strike-slip fault systems. *American Association of Petroleum Geologists Bulletin*, **85**, 233–260.

Mizerski, W. 1991. Ewolucja tektoniczna regionu łysogórskiego Gór Świętokrzyskich. Rozprawy UW, 362, 1–141.

Mizerski, W. and Orłowski, S. 1993. Główne uskoki poprzeczne i ich znaczenie dla tektoniki antyklinorium klimontowskiego – Góry Świętokrzyskie. *Geological Quarterly*, **37**, 19–40.

Moody, J.D. and Hill, M.J. 1956. Wrench–fault tectonics. *Geological Society of America Bulletin*, **67**, 1207–1246.

Morley, C.K., Kongwung, B., Julapour, A.A., Abdolghafourian, M., Hajian, M., Waples, D.,Warren, J., Otterdoom, H., Srisuriyon, K. and Kazemi, H. 2009. Structural development of a major late Cenozoic basin and transpressional belt in central Iran: the Central Basin in the Qom-Saveh area. *Geosphere*, **5**, 1–38.

Nadimi, A. and Konon, A. 2012. Strike-slip faulting in the central part of the Sanandaj–Sirjan Zone, Zagros Orogen Iran. *Journal of Structural Geology*, **40**, 2–16.

Narkiewicz, M., Resak, M., Littke, R. and Marynowski, L. 2010. New constraints on the Middle Palaeozoic to Cenozoic burial and thermal history of the Holy Cross Mts. (Central Poland): results from numerical modelling. *Geologica Acta*, **8**, 189–205.

Oglesby, D.D. 2005. The dynamics of strike-slip step-overs with linking dip-slip faults. *Bulletin of the Seismological Society of America*, **95**, 1604–1622.

Pánek, T., Tábořík, P., Klimeš, J., Komárková, V., Hradecký, J. and Šťastný, M. 2011. Deep-seated gravitational slope deformations in the highest parts of the Czech Flysch Carpathians: Evolutionary model based on kinematic analysis, electrical imaging and trenching. *Geomorphology*, **129**, 92–112.

Peacock, D.C.P., Anderson, M.W., Morris, A. and Randall, D.E. 1998. Evidence for the importance of 'small' faults on block rotation. *Tectonophysics*, **299**, 1–13.

Pieńkowski, G. 1991. Eustatically-controlled sedimentation in the Hettangian–Sinemurian (Early Jurassic) of Poland and Sweden. *Sedimentology*, **38**, 503–518.

Pieńkowski, G. 2004. The epicontinental Lower Jurassic of Poland. *Polish Geological Institute Special Papers*, **12**, 1–154.

Piwocki, M. 2004. Paleogen. In: T.M. Peryt and M. Piwocki (Eds), Budowa geologiczna Polski. T. I, cz.3a: Stratygrafia. Kenozoik, Paleogen, Neogen, pp. 22–71. Państwowy Instytut Geologiczny; Warszawa.

Pożaryski, W. 1964. Outline of Palaeozoic and Mesozoic tectonics of the Polish Lowland. *Kwartalnik Geologiczny*, **8**, 1–41. [In Polish with English summary]

Pożaryski, W. 1976. Położenie mezozoiku świętokrzyskiego na tle geologii Europy Środkowej. In: W. Pożaryski (Ed.), Przewodnik 48 Zjazdu Polskiego Towarzystwa Geologicznego, pp. 7–13. Starachowice.

Pożaryski, W. and Brochwicz-Lewiński, W. 1979. O aulakogenie środkowopolskim, *Kwartalnik Geologiczny*, **23**, 271–290.

Radwański, A. 1969. Lower Tortonian transgression onto the southern slopes of the Holy Cross Mts. *Acta Geologica Polonica*, **19**, 1–164.

Radwański, A. 1973. Transgresja dolnego tortonu na południowo–wschodnich i wschodnich stokach Gór Świętokrzyskich. *Acta Geologica Polonica*, **23**, 375–434.

Radwański, A. and Górka, M. 2012. Wybrzeże morza mioceńskiego – Korytnica, Lubania i głazowisko klifowe w Skotnikach. In: S. Skompski (Ed.), Góry Świętokrzyskie. 25 najważniejszych odsłonięć geologicznych. Uniwersytet Warszawski, Wydział Geologii, 131–137. Warszawa.

Riedel, W. 1929. Zur Mechanik Geologischer Brucherscheinungen. *Zentrablatt für Mineralogie, Geologie und Paläontologie, B*, 354–368.

Różycki, S.Z. 1961. Materiały do przeglądowej mapy geologicznej Polski. Region Świętokrzyski. Arkusz Włoszczowa. Wyd. B zaktualizowane, skala 1:100 000. Wydawnictwa Geologiczne; Warszawa.

Rybak-Ostrowska, B., Konon, A. and Domonik, A. 2015. Wpływ litologii na deformacje skał osadowych w strefach uskokowych przesuwczych (Góry Świętokrzyskie).

In: S. Skompski, W. Mizerski (Eds), Przewodnik 84 Zjazdu Naukowego Polskiego Towarzystwa Geologicznego, pp. 101–102. Państwowy Instytut Geologiczny – PIB; Warszawa.

Rybak-Ostrowska, B., Konon, A., Domonik, A., Poszytek, A. and Uroda J. 2016. Shallow-generated damage within non-planar strike-slip fault zones: role of sedimentary rocks in slip accommodation, SW Holy Cross Mountains, Poland. *International Journal of Earth Science*s (*Geologische Rundschau*) doi:10.1007/s00531-016-1390-4

Segall, P. and Pollard, D.D. 1980. Mechanics of discontinuous faults. *Journal of Geophysical Research: Solid Earth*, **85**, 4337–4350.

Senkowicz, E. 1959. The Jurassic and Cretaceous between Jędrzejów and the Nida river. *Biuletyn Instytutu Geologicznego*, **159**, 107–149. [In Polish with English summary]

Senkowiczowa, H. 1961. The Röth and Muschelkalk on the southern slope of the Święty Krzyż Mts. between Czarna Nida and Chmielnik. *Biuletyn Instytutu Geologicznego*, **167**, 41–89. [In Polish with English summary]

Scheck, M., Bayer, U., Otto, V., Lamarche, J., Banka, D. and Pharaoh, T. 2002. The Elbe Fault System in North Central Europe – a basement controlled zone of crustal weakness. *Tectonophysics*, **360**, 281–299.

Scheck, M. and Lamarche, J. 2005. Crustal memory and basin evolution in the Central European Basin System – new insights from a 3D structural model. *Tectonophysics*, **397**, 143–165.

Shebalin, N.V., Leydecker, G., Mokrushina, N.G., Tatevossian, R.E., Erteleva, O.O. and Vassiliev V.Yu. 1998. Earthquake Catalogue For Central And Southeastern Europe 342 Bc –1990 Ad, 1–50, Final Report to Contract ETNUCT93-0087 (with appendixes), Brussels, Belgium.

Siemiątkowska–Giżejewska, M. 1974. Stratigraphy and paleontology of Callovian in the southern and western margins of the Holy Cross Mts. *Acta Geologica Polonica*, **24**, 365–406.

Stampfli, G.M., Borel, G., Cavazza, W., Mosar, J. and Ziegler, P.A. (Eds). 2001. The Paleotectonic Atlas of the PeriTethyan Domain (CD–ROM): European Geophysical Society.

Stupnicka, E. 1972. Tektonika południowo–zachodniego obrzeżenia Gór Świętokrzyskich. *Biuletyn Geologiczny Uniwersytetu Warszawskiego*, **14**, 21–114.

Sylvester, A.G. 1988. Strike slip faults. *Geological Society of America Bulletin*, **100**, 1666–1703.

Szajn, J. 1977. Geological Map of Poland, Nagłowice sheet (849), scale 1:50 000. Wydawnictwa Geologiczne; Warszawa.

Szajn, J. 1980. Geological Map of Poland, Włoszczowa sheet (812), scale 1:50 000. Wydawnictwa Geologiczne; Warszawa.

Szajn, J. 1983. Geological Map of Poland, Oleszno sheet (813), scale 1:50 000. Wydawnictwa Geologiczne; Warszawa.

Szajn, J. 1984. Explanations to Geological Map of Poland, Oleszno sheet (813), scale 1:50 000. Wydawnictwa Geologiczne; Warszawa.

Szaniawski, R., Konon, A., Grabowski, J. and Schnabl, P. 2011. Palaeomagnetic age constraints on folding and faulting events in Devonian carbonates of the Kielce fold zone (southern Holy Cross Mountains, Central Poland). *Geological Quarterly*, **55**, 223–234.

Świdrowska, J. 2007. Kreda w regionie lubelskim – sedymentacja i jej tektoniczne uwarunkowania. *Biuletyn Państwowego Instytutu Geologicznego*, **422**, 63–78.

Świdrowska, J., Hakenberg, M., Poluhtovič, B., Seghedi, A. and Višnâkov, I. 2008. Evolution of the Mesozoic Bains on the southwestern edge of the East European Craton (Poland, Ukraine, Moldova, Romania). *Studia Geologica Polonica*, **130**, 3–130.

Terrizzano, C.M., Fazzito, S.Y., Cortés, J.M. and Rapalini, A.E. 2010. Studies of Quaternary deformation zones through geomorphic and geophysical evidence: A case in the Precordillera Sur, Central Andes of Argentina. *Tectonophysics*, **490**, 184–196.

Terrizzano, C.M., Fazzito, S.Y., Cortés, J.M. and Rapalini, A.E. 2012. Electrical resistivity tomography applied to the study of neotectonic structures, northwestern Precordillera Sur, Central Andes of Argentina. *Journal of South American Earth Sciences*, **34**, 47–60.

Vialon, P.P. 1979. Les déformations continues–discontinues des roches anisotropes. *Eclogae Geologicae Helvetiae*, **72**, 531–549.

Wakabayashi, J. 1999. Distribution of displacement on, and evolution of, a young transform fault system: the northern San Andreas fault system, California. *Tectonics*, **18**, 1245–1274.

Wakabayashi, J. 2007. Stepovers that migrate with respect to affected deposits: field characteristics and speculation on some details of their evolution. In: W.D. Cunningham, and P. Mann (Eds), Tectonics of Strike-Slip Restraining and Releasing Bends. *Geological Society, London, Special Publications*, **290**, 169–188.

Wakabayashi, J., Hengesh, J.V. and Sawyer, T.L. 2004, Four-dimensional transform fault processes: progressive evolution of step-overs and bends. *Tectonophysics*, **392**, 279–301.

Wilcox, R.E., Harding, T.P. and Seely, D.R. 1973, Basic wrench tectonics. *American Association of Petroleum Geologists Bulletin*, **57**, 74–96.

Woodcock, N.H. and Fisher, M. 1986. Strike-slip du-

plexes. *Journal of Structural Geology*, **8**, 725–735.

Woodcock, N.H. and Schubert, C. 1994. Continental strike-slip tectonics. In: P.L. Hancock (Ed.), Continental Deformation, pp. 251–263. Pergamon Press; Oxford.

Woodcock, N.H. and Rickards, B. 2003. Transpressive duplex and flower structure: Dent Fault System, NW England. *Journal of Structural Geology*, **25**, 1981–1992.

Ziegler, P.A. 1982. Geological Atlas of Western and Central Europe, pp. 1–130. Elsevier; Amsterdam.

Ziegler, P.A. 1987. Late Cretaceous and Cenozoic intra-plate compressional deformations in the Alpine foreland – a geodynamic model. *Tectonophysics*, **137**, 389–420.

Ziegler, P.A. 1990a. Collision related intra-plate compression deformations in Western and Central Europe. *Journal of Geodynamics*, **11**, 357–388.

Ziegler, P.A. 1990b. Geological Atlas of Western and Central Europe, pp. 1–239. Shell Internationale Petroleum Mij. BV and Geological Society of London. [2nd ed.]

Zoback, M.L., Jachens, R.C. and Olson, J.A. 1999. Abrupt along strike change in the tectonic style: San Andreas fault zone, San Francisco peninsula. *Journal of Geophysical Research,* **104**, 10719–10742.

Zuchiewicz, W., Badura, J. and Jarosiński, M. 2007. Neotectonics of Poland: an overview of active faulting. *Studia Quaternaria*, **24**, 5–20.